References

1 Takeiri A, Mishima M, Tanaka K, Shioda A, Harada A, Watanabe K, Masumura K, Nohmi T. A newly established GDL1 cell line from *gpt* delta mice well reflects the *in vivo* mutation spectra induced by mitomycin C. Mutat Res. 2006; 609: 102–15.

2 Loehrer PJ, Einhorn LH. Drugs five years later. Cisplatin. Ann Intern Med. 1984; 100: 704–13.

3 Rosenberg B. Fundamental studies with cisplatin. Cancer. 1985; 55: 2303–16.

4 Burnouf D, Daune M, Fuchs RP. Spectrum of cisplatin-induced mutations in *Escherichia coli*. Proc Natl Acad Sci USA. 1987; 84: 3758–62.

5 Cariello NF, Swenberg JA, Skopek TR. *In vitro* mutational specificity of cisplatin in the human hypoxanthine guanine phosphoribosyltransferase gene. Cancer Res. 1992; 52: 2866–73.

6 Yarema KJ, Lippard SJ, Essigmann JM. Mutagenic and genotoxic effects of DNA adducts formed by the anticancer drug *cis*-diamminedichloroplatinum(II). Nucleic Acids Res. 1995; 23: 4066–72.

7 Louro H, Silva MJ, Boavida MG. Mutagenic activity of cisplatin in the *lacZ* plasmid-based transgenic mouse model. Environ Mol Mutagen. 2002; 40: 283–91.

8 Plooy AC, Lohman PH. Platinum compounds with antitumour activity. Toxicology. 1980; 17: 169–76.

9 Johnson NP, Hoeschele JD, Rahn RO, O'Neill JP, Hsie AW. Mutagenicity, cytotoxicity, and DNA binding of platinum(II)chloroammines in Chinese hamster ovary cells. Cancer Res. 1980; 40: 1463–8.

10 Plooy AC, van Dijk M, Lohman PH. Induction and repair of DNA crosslinks in Chinese hamster ovary cells treated with various platinum coordination compounds in relation to platinum binding to DNA, cytotoxicity, mutagenicity, and antitumor activity. Cancer Res. 1984; 44: 2043–51.

11 Gebel T, Lantzsch H, Plessow K, Dunkelberg H. Genotoxicity of platinum and palladium compounds in human and bacterial cells. Mutat Res. 1997; 389: 183–90.

12 Pestell KE, Hobbs SM, Titley JC, Kelland LR, Walton MI. Effect of p53 status on sensitivity to platinum complexes in a human ovarian cancer cell line. Mol Pharmacol. 2000; 57: 503–11.

13 Lantzsch H, Gebel T. Genotoxicity of selected metal compounds in the SOS chromotest. Mutat Res. 1997; 389: 191–7.

14 Nishi Y, Hasegawa MM, Taketomi M, Ohkawa Y, Inui N. Comparison of 6-thioguanine-resistant mutation and sister chromatid exchanges in Chinese hamster V79 cells with forty chemical and physical agents. Cancer Res. 1984; 44: 3270–9.

15 Eastman A. Characterization of the adducts produced in DNA by *cis*-diamminedichloroplatinum(II) and *cis*-dichloro(ethylenediamine)platinum(II). Biochemistry. 1983; 22: 3927–33.

16 Eastman A. Reevaluation of interaction of *cis*-dichloro(ethylenediamine)platinum(II) with DNA. Biochemistry. 1986; 25: 3912–5.

17 Brabec V, Leng M. DNA interstrand crosslinks of *trans*-diamminedichloroplatinum(II) are preferentially formed between guanine and complementary cytosine residues. Proc Natl Acad Sci USA. 1993; 90: 5345–9.

18 Boudvillain M, Dalbiès R, Aussourd C, Leng M. Intrastrand crosslinks are not formed in the reaction between transplatin and native DNA: relation with the clinical inefficiency of transplatin. Nucleic Acids Res. 1995; 23: 2381–8.

19 Brouwer J, van de Putte P, Fichtinger-Schepman AM, Reedijk J. Base-pair substitution hotspots in GAG and GCG nucleotide sequences in *Escherichia coli* K-12 induced by *cis*-diamminedichloroplatinum (II). Proc Natl Acad Sci USA. 1981; 78: 7010–4.

20 Burnouf D, Gauthier C, Chottard JC, Fuchs RP. Single d (ApG) / *cis* - diamminedichloroplatinum (II) adduct-induced mutagenesis in *Escherichia coli*. Proc Natl Acad Sci USA. 1990; 87: 6087–91.

21 Bubley GJ, Ashburner BP, Teicher BA. Spectrum of *cis*-diamminedichloroplatinum(II)-induced mutations in a shuttle vector propagated in human cells. Mol Carcinog. 1991; 4: 397–406.

22 Silva MJ, Costa P, Dias A, Valente M, Louro H, Boavida MG. Comparative analysis of the mutagenic activity of oxaliplatin and cisplatin in the *Hprt* gene of CHO cells. Environ Mol Mutagen. 2005; 46: 104–15.

23 Roberts JJ, Friedlos F. Differential toxicity of *cis*- and *trans*-diamminedichloroplatinum(II) toward mammalian cells: lack of influence of any difference in the rates of loss of their DNA-bound adducts. Cancer Res. 1987; 47: 31–6.

24 Chu G. Cellular responses to cisplatin. The roles of DNA-binding proteins and DNA repair. J Biol Chem. 1994; 269: 787–90.

25 Masumura K, Kuniya K, Kurobe T, Fukuoka M, Yatagai F, Nohmi T. Heavy-ion-induced mutations in the *gpt* delta transgenic mouse: Comparison of mutation spectra induced by heavy-ion, X-ray, and gamma-ray radiation. Environ Mol Mutagen. 2002; 40: 207–15.

26 Takeiri A, Mishima M, Tanaka K, Shioda A, Ueda O, Suzuki H, Inoue M, Masumura K, Nohmi T. Molecular characterization of mitomycin C-induced large deletions and tandem-base substitutions in the bone marrow of *gpt* delta transgenic mice. Chem Res Toxicol. 2003; 16: 171–9.

27 Carr GJ, Gorelick NJ. Mutational spectra in transgenic animal research: data analysis and study design based upon the mutant or mutation frequency. Environ Mol Mutagen. 1996; 28: 405–13.

28 Yarema KJ, Wilson JM, Lippard SJ, Essigmann JM. Effects of DNA adduct structure and distribution on the mutagenicity and genotoxicity of two platinum anticancer drugs. J Mol Biol. 1994; 236: 1034–48.

29 de Boer JG, Glickman BW. Sequence specificity of mutation induced by the anti-tumor drug cisplatin in the CHO *aprt* gene. Carcinogenesis. 1989; 10: 1363–7.

30 Pinto AL, Lippard SJ. Sequence-dependent termination of *in vitro* DNA synthesis by *cis*- and *trans*-diamminedichloroplatinum(II). Proc Natl Acad Sci USA. 1985; 82: 4616–9.

31 Bernal-Méndez E, Boudvillain M, González-Vílchez F, Leng M. Chemical versatility of transplatin monofunc-

tional adducts within multiple site-specifically platinated DNA. Biochemistry. 1997; 36: 7281–7.

32 Zwelling LA, Bradley MO, Sharkey NA, Anderson T, Kohn KW. Mutagenicity, cytotoxicity and DNA cross-linking in V79 Chinese hamster cells treated with *cis*- and *trans*-Pt(II) diamminedichloride. Mutat Res. 1979; 67: 271–80.

33 Pascoe JM, Roberts JJ. Interactions between mammalian cell DNA and inorganic platinum compounds. II. Interstrand crosslinking of isolated and cellular DNA by platinum(IV) compounds. Biochem Pharmacol. 1974; 23: 1345–57.

34 Ohta T, Ohmae S, Yamaya K, Kanemichi Y, Tokishita S, Yamagata H. Characterization of the mutational specificity of DNA crosslinking mutagens by the Lac$^+$ reversion assay with *Escherichia coli*. Teratog Carcinog Mutagen. 2001; 21: 275–82.

35 Hefferin ML, Tomkinson AE. Mechanism of DNA double-strand break repair by non-homologous end joining. DNA Repair. 2005; 4: 639–48.

New Insight into Intrachromosomal Deletions Induced by Chrysotile in the *gpt* delta Transgenic Mutation Assay

An Xu,[1,2] Lubomir B. Smilenov,[1] Peng He,[1] Ken-ichi Masumura,[3] Takehiko Nohmi,[3] Zengliang Yu,[2] and Tom K. Hei[1,4]

[1]Center for Radiological Research, College of Physicians & Surgeons, Columbia University, New York, New York, USA; [2]Key Laboratory of Ion Beam Bioengineering, Institute of Plasma Physics, Chinese Academy of Sciences, Hefei, Anhui, People's Republic of China; [3]Division of Genetics and Mutagenesis, National Institute of Health Sciences, Tokyo, Japan; [4]Department of Environmental Health Sciences, Mailman School of Public Health, Columbia University, New York, New York, USA

BACKGROUND: Genotoxicity is often a prerequisite to the development of malignancy. Considerable evidence has shown that exposure to asbestos fibers results in the generation of chromosomal aberrations and multilocus mutations using various *in vitro* approaches. However, there is less evidence to demonstrate the contribution of deletions to the mutagenicity of asbestos fibers *in vivo*.

OBJECTIVES: In the present study, we investigated the mutant fractions and the patterns induced by chrysotile fibers in *gpt* delta transgenic mouse primary embryo fibroblasts (MEFs) and compared the results obtained with hydrogen peroxide (H_2O_2) in an attempt to illustrate the role of oxyradicals in fiber mutagenesis.

RESULTS: Chrysotile fibers induced a dose-dependent increase in mutation yield at the *redBA/gam* loci in transgenic MEF cells. The number of λ mutants losing both *redBA* and *gam* loci induced by chrysotiles at a dose of 1 μg/cm^2 increased by > 5-fold relative to nontreated controls ($p < 0.005$). Mutation spectra analyses showed that the ratio of λ mutants losing the *redBA/gam* region induced by chrysotiles was similar to those induced by equitoxic doses of H_2O_2. Moreover, treatment with catalase abrogated the accumulation of γ-H2AX, a biomarker of DNA double-strand breaks, induced by chrysotile fibers.

CONCLUSIONS: Our results provide novel information on the frequencies and types of mutations induced by asbestos fibers in the *gpt* delta transgenic mouse mutagenic assay, which shows great promise for evaluating fiber/particle mutagenicity *in vivo*.

KEY WORDS: chrysotile asbestos, *gpt* delta transgenic mutation system, kilobase-sized mutation, oxyradicals, γ-H2AX. *Environ Health Perspect* 115:87–92 (2007). doi:10.1289/ehp.9425 available via *http://dx.doi.org/* [Online 6 September 2006]

Asbestos fibers, a group of naturally occurring silicate minerals, are well-established human carcinogens. They are causally related to the development of asbestosis, bronchial carcinoma, malignant mesothelioma of the pleura and peritoneum, and possibly cancers of the gastrointestinal tract and larynx (Gustavsson et al. 1998; International Agency for Research on Cancer 1987). Although the main concern of asbestos-related diseases focuses primarily on the workplace, the danger of developing such diseases now extends beyond that of a simple occupational hazard because accumulating evidence suggests that asbestos fibers are widely distributed in the environment to which the general public may be exposed (Gardner and Saracci 1989). Individuals may be subjected to prolonged exposure to asbestos in their homes, schools, drinking water, neighborhoods of industrial sources of asbestos, or areas of a natural occurring asbestos (Kjaerheim et al. 2005; Miller 2005; Rom et al. 2001). Recent evidence indicates an excess risk of mesothelioma in individuals living in the vicinity of a natural occurring source of asbestos (Pan et al. 2005). The continued discovery of routes through which the general public may be exposed to asbestos suggests a long-term, low-level exposure of a large number of people, which may lead to an elevated risk of asbestos-related diseases.

The mechanisms by which asbestos produces malignancy are unclear at present. It has been reported that fiber dimension, biopersistence, composition, surface reactivity, and physical durability are important criteria for the carcinogenicity of the fibers, indicating that carcinogenic mechanisms of asbestos are likely to be complex and involve multiple pathways (Bernstein et al. 2003; Coin et al. 1994). Various highly quantitative genotoxicity assays ranging from DNA strand breaks to gene mutations in rodent cells have been performed to estimate the carcinogenic potential of asbestos fibers (Lezon-Geyda et al. 1996; Poser et al. 2004). Although asbestos fibers have been shown to induce chromosomal aberrations and sister chromatid exchanges, mutagenic studies at the hypoxanthine–guanine phosphoribosyl transferase (*hprt*; GenBank accession no. NM_013556; http://www.ncbi.nlm.nih.gov/) and ouabain loci in mammalian cells have been shown to be either inactive or weakly active (Jaurand 1996). Using the human–hamster hybrid cell line (A_L) in which mutations are scored at a marker gene (*CD59*) located on human chromosome 11 (11p13) that the A_L cell carries as its only human chromosome, our previous studies have demonstrated that asbestos fibers are indeed mutagenic and induce mostly deletions involving millions of base pairs (Hei et al. 1992). In contrast, among the same fiber-treated A_L cell population, there are few, if any, mutations scored at the *hprt* locus of the hamster X chromosome. This discrepancy has been attributed to the possibility that the *hprt* gene is located on the X chromosome, and large deletions in the region of the gene that are required for cell survival would be lethal and any mutants induced would not be viable. In recent years several other mutagenic assays that are proficient in detecting either large deletions, homologous recombinations, or score mutants located in nonessential genes have been used successfully to demonstrate the mutagenic potential of various fiber types (Lezon-Geyda et al. 1996; Park and Aust 1998). These findings provide a direct link between chromosomal abnormalities that frequently have been demonstrated in fiber exposed human and rodent cell lines and carcinogenicity *in vivo*. However, there is less direct evidence that illustrates chromosomal mutations of asbestos fibers in various organs and tissues in intact organisms.

The use of transgenic mouse systems carrying bacterial reporter genes such as *lacZ*, *lacI*, and *cII* has opened a promising opportunity for short-term mutagenicity analysis (Dean et al. 1999). There is evidence to show that asbestos fibers are mutagenic and induce point mutations in either Big Blue transgenic mice or rats bearing λ-*lacI* as a reporter gene (Rihn et al. 2000; Topinka et al. 2004; Unfried et al. 2002). However, most genome-wide mutations such as large deletions, insertions, translocations, and aneuploidy are not effectively recovered by the *lacI* shuttle vector. To efficiently recover large deletions *in vivo*, *gpt* (xanthine phosphoribosyltransferase;

Address correspondence to T.K. Hei, Center for Radiological Research, Columbia University, New York, NY 10032 USA. Telephone: (212) 305-8462. Fax: (212) 305-3229. E-mail: TKH1@Columbia.edu

We thank M. Partridge and V. Ivanov for their critical reading of the manuscript and R. Baker for his technical assistance with Spi$^-$ detection.

Work was supported in part by National Institutes of Health grant ES 05786, Superfund grant ES 10349, National Institute of Environmental Health Sciences Center grant ES 09089, and National Nature Science Foundation of China grant 20322202.

The authors declare they have no competing financial interests.

Received 14 June 2006; accepted 6 September 2006.

GenBank accession no. NP_414773; http://www.ncbi.nlm.nih.gov/GenBank) delta transgenic mice have been established by integrating multiple copies of λ EG10 DNA with the *redBA* and *gam* (Genbank accession no. J02459; http://www.ncbi.nlm.nih.gov/GenBank) genes into each chromosome 17 of C57BL/6J mice (Nohmi and Masumura 2004). Because wild-type λ-phage DNA replicate poorly in the presence of P2 lysogens in the host cells (called "sensitive to P2 interference" or "Spi"), only mutant λ phages that are deficient in the functions of both the *redBA* and *gam* genes are able to escape from P2 interference (called "Spi⁻") and form visible clear plaques on a bacterial lawn. Simultaneous inactivations of both the *redBA* and *gam* genes, an indication of deletions in the gene loci region, provide an available method to quantify deletion mutations induced by various physical and chemical mutagens, such as X rays and alkylating agents (Horiguchi et al. 2001; Shibata et al. 2005).

Chrysotile asbestos, a fibrous serpentine, is the most commercially used form of asbestos in the world trade and accounts for > 95% of asbestos found in United States buildings. In the present study we adapted the *gpt* delta transgenic mouse mutation system to evaluate the genotoxicity of chrysotile in *gpt* delta mouse primary embryo fibroblast (MEF) cells. We investigated the mutation frequencies at both *redBA* and *gam* (GenBank accession no. J02459; http://www.ncbi.nlm.nih.gov/GenBank) loci and the contribution of deletions > 2 kb to the mutagenicity of chrysotile fibers. Because reactive oxygen species (ROS) such as superoxide anions (O_2^-) and hydrogen peroxide (H_2O_2) originate not only from redox reactions catalyzed on the fiber surface but also from the incomplete phagocytosis of fibers in various cells, such as phagocytic, mesothelial, and rat lung epithelium cells, we speculated that asbestos fibers would induce similar types of mutations as that of chemically generated oxyradicals. We found that both chrysotile and H_2O_2 dramatically increased the mutation yield, which could be abrogated by concurrent treatment with catalase. Furthermore, the ratios of mutants with deletions > 2 kb were similar to those generated by oxyradicals at two equitoxic doses. The accumulation of phosphorylated histone H2AX (γ-H2AX) further demonstrated the involvement of DNA double-strand break (DSB) in the mutagenicity of chrysotiles. These results provide direct evidence that asbestos fibers induced kilobase pair deletion mutations in a transgenic mouse mutation system, and that these were mediated by oxyradicals.

Materials and Methods

MEF cell culture. *gpt* delta transgenic mice, obtained from T. Nohmi, were mated, and pregnant females were sacrificed on day 14 of the experimental protocol were previously approved by the Columbia University Institutional Animal Care and Use Committee. The animals were treated humanely and with regard for the alleviation of pain and suffering. The embryos were surgically removed and embryonic tissue prepared in culture according to standard procedures (Hogan et al. 1994). These cultures were grown and maintained in Dulbecco's modified Eagle's medium (Gibco-BRL, Gaithersburg, MD, USA) containing 15% heat-inactivated fetal bovine serum and penicillin (100 U/mL), streptomycin (50 μg/mL) in a 5% CO_2 environment at 37°C.

Chrysotile preparation. We used International Union Against Cancer standard reference chrysotile asbestos (average length, 7.8 μm; average diameter, 0.2 μm) in these studies (Timbrell 1979). The fibers were prepared as described previously (Hei et al. 1992). Briefly, samples of fibers were weighed and suspended in distilled water. The fiber suspension was triturated 6–8 times with a 20-gauge syringe needle. A stock solution of the fibers was sterilized by autoclaving and mixed to ensure a uniform suspension before being diluted with tissue culture medium for cell treatment.

Cytotoxicity assay. We evaluated cell viability using MTT (3-(4,5-dimethylthiazol-2-yl)-2,5-diphenyltetrazolium bromide) assay on the basis of the ability of viable cells to convert a water-soluble tetrazolium salt into a water-insoluble formazan product (Scudiero et al. 1988). The enzymatic reduction of the tetrazolium salt happens only in living, metabolically active cells but not in dead cells. Cultures were incubated in two-well chamber slides at a density of 1.0×10^5 cells per well at 37°C for 24 hr. Graded doses of either chrysotile or H_2O_2 were added to the culture medium and incubated for another 24 hr in the presence of serum (chrysotile) or 15 min in the absence of serum (H_2O_2). At the end of the treatment period, the medium was removed, 200 μL of 5 mg/mL MTT was added to each well, and the cultures were incubated for another 4 hr. The supernatant was removed and 1 mL acidic isopropanol was added to dissolve the formazan crystals. The absorbance at 570 nm was determined by an Ultrospec 3100 pro UV/Visible spectrophotometer (Biochrom Ltd., Cambridge, UK).

Genomic DNA isolation. We isolated genomic DNA from MEF cells using the RecoverEase DNA isolation kit (Stratagene, La Jolla, CA, USA) according to the protocol developed by the supplier. Briefly, about 5.0×10^6 cells were transferred to a chilled Wheaton dounce tissue grinder (Fisher, Hampton, NH, USA), and the homogenate obtained was filtered and centrifuged at 1,100 × *g* for 12 min at 4°C. The pellet was resuspended in digestion buffer containing RNAses (RANse-It; Stratagene) containing proteinase K solution (2 mg/mL prewarmed to 50°C). Using wide-bore pipette tips, the samples were transferred to dialysis cups floating on the surface of TE buffer (500 mL) and dialyzed for 24 hr. The purity and concentration of DNA was checked spectrophotometrically and samples were diluted with TE [10 mM Tris–Cl (pH 7.5), 1 mM EDTA] buffer to a final DNA concentration of approximately 0.5 mg/mL, and stored at 4°C for up to 3 months prior to mutation analysis.

In vitro packaging of DNA. The λ DNA was recovered from approximately 5 μg genomic DNA and packaged with terminase and phage proteins contained in the Transpack kit (Stratagene) to produce infectious λ phages. Viable phages were infected into *Escherichia coli* XL-1 Blue MRA (Stratagene), mixed with λ-trypticase agarose and poured onto 100-mm plates containing 30 mL bottom agar. Plates were incubated overnight at 37°C. The average of rescued phages per packaging reaction was 1.8×10^6 in the present studies. There was no significant difference in the titers between control and exposed groups.

Spi⁻ mutation analysis. The mutant frequencies at *red/gam* loci were determined by Spi⁻ selection as described previously (Nohmi and Masumura 2004; Nohmi et al. 1996; Shibata et al. 2005). Briefly, packaged phages were infected into *E. coli* XL-1 Blue MRA (P2) (Stratagene). Infected cells were mixed with molten soft agar, poured onto λ-trypticase agar plates and incubated at 37°C. The plaques detected on the plates (Spi⁻ candidates) were suspended in 50 μL of SM buffer [0.58% NaCl, 0.2% $MgSO_4 \cdot 7H_2O$, 50 mM Tris–HCl, 0.01% gelatin (pH 7.5)]. The suspension was spotted on the two types of plates where *E. coli* XL-1 Blue MRA (P2) or WL95 (P2) strain was spread. The plates were incubated for 24 hr at 37°C. The numbers of mutants that made clear spots on both strains

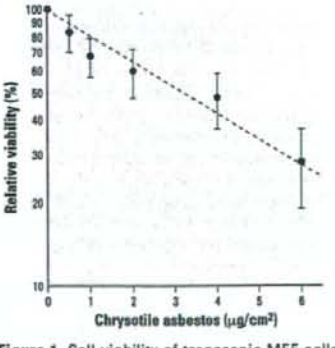

Figure 1. Cell viability of transgenic MEF cells treated with graded doses of chrysotile for 24 hr. Data were the average of three independent experiments. Error bars indicate ± SD.

were counted as confirmed Spi⁻ mutants. Mutation frequencies were calculated by comparing the titration and number of confirmed mutant plaques.

Spi⁻ mutant characterization. To determine the mutated region, the phage DNA was used and subjected to DNA sequence and polymerase chain reaction (PCR) analysis with various sets of primers (Horiguchi et al. 2001). The PCR primers used were as follows: primer 1: 5′-CACTCTCTTT GATGCGAATGCCAGCGTCAGAC-3′; primer 2: 5′-CAGGAGTAATTATGCG GAACAGAATCATGCCTGGTG-3′; primer 3: 5′-GTGAGGATGCGTCATCGCCAT TGCTCCCC-3′; primer 4: 5′-GCGATGA AAAGATGTTTCGTGAAGCCGTC GACGC-3′; primer 5: 5′-AAACAGGCG CGGGCATCAGCGTGGTCTGA-39′; primer 12: 5′-CGCGCGGTCGAGGGACC TAATAACTTCGTA-3′. We performed PCR amplification under the following conditions: 4 µL of phage DNA, 0.2 mM each dNTP, 1.5 mM $MgCl_2$, Taq DNA polymerase (or ExTaq; Takara Shuzo Co., Kyoto, Japan), and 20 pmol of each primer in a 40-µL reaction volume; heating for 1–2 min at 94°C, and 24 cycles at 98°C for 20 sec and at 68°C for X minutes (1 min/1 kb), followed by final extension at 72°C for 10 min. The products were analyzed using agarose gel electrophoresis.

The PCR products were sequenced by ABI's 3100 capillary sequencers (Dye Terminator Cycle Sequencing; PE Applied Biosystems, Foster City, CA, USA). PCR products for templates of sequence were purified using PCR product presequencing kit (Amersham Life Science, Piscataway, NJ, USA).

Sequence primers are as follows: s102: 5′-AATCCAAACTCTTTACCCGTCCTT GGGT-3′; s201: 5′-CGCTTGATAACTCT GTTGAATGGCTCT-3′; s301: 5′-GGTGG AATCCCATCAGCGTTACCGTTT-3′; s302: 5′-AGTGATTGCGCCTACCCG GATATTATCGTG-3′; s403: 5′-CCAGC CGACACGTTCAGCCAGCTTCCCAG-3′. The entire DNA sequence of λ EG10 is available at http://dgm2alpha.nihs.go.jp (Masumura et al. 2003).

Determination of H2AX phosphorylation using flow cytometry. The cells were fixed by adding 2% paraformaldehyde dropwise while being vortexed. The fixed cells were then stained with mouse monoclonal anti–γ-H2AX (Upstate, Lake Placid, NY, USA) and fluorescein isothiocyanate (FITC)–conjugated secondary antibodies (Sigma-Aldrich Chemical Co., St. Louis, MO, USA) as described by Kurose et al. (2005). The cells were then suspended in 0.5 mL of 10 µg/mL propidium iodide (PI) and 40 µg/mL RNase A and incubated at 4°C for at least 30 min. The fluorescence of PI and FITC of individual cells induced by excitation with a 488-nm argon ion laser was measured using a FACSCalibur cytometer (BD Biosciences, San Jose, CA).

Statistical analysis. All numerical data were calculated as mean and SD and evaluated by Student's *t*-test. The statistical significance was tested at $p < 0.05$ as the critical value.

Results

Chrysotile-induced dose-dependent toxicity in transgenic MEF cells. The viability of MEF cells exposed to graded doses of chrysotile was analyzed by using the MTT assay. As shown in Figure 1, exposure of MEF cells to doses of chrysotiles ranging from 0.5 to 6 µg/cm² for 24 hr produced a dose-dependent decrease in cell viability. The viabilities of MEF cells was reduced by 14, 29, and 59%, when the concentrations of chrysotile were 0.5, 1, and 2 µg/cm², respectively. The median lethal dose of chrysotile, which resulted in 50% cell killing, was approximately 3.2 µg/cm².

Mutation frequencies at red/gam *gene loci were elevated in response to chrysotile exposure.* We have shown previously that asbestos is mutagenic and induces multilocus deletions in mammalian cells (Hei et al. 1992). To investigate the mutagenicity of asbestos in the *gpt* delta assay, we used an Spi⁻ mutation assay to determine the mutation frequencies induced by chrysotile exposure in transgenic MEF cells. The average number of spontaneous *red/gam* gene mutants per 10^6 recovered plaques in MEF cells used for these experiments was 4.69 ± 1.80. Treatment of MEF cells with chrysotile fibers resulted in a dose-dependent induction of mutation yield at the *red/gam* gene locus (Figure 2). A significant increase in mutation yield over the background level was observed at fiber concentrations > 1 µg/cm² ($p < 0.005$). The mutant fraction in cells treated with a dose of 1 µg/cm² of fibers was 2.4-fold higher than background. These results indicated that chrysotile asbestos were able to produce deletion mutations in *gpt* delta transgenic mutation assay system.

Characterization of mutant spectra induced by chrysotile. To determine the spectrum of mutations induced by chrysotile fibers, 93 and 74 λ mutants from control cells and cells treated with chrysotile at 1 µg/cm², respectively, were subjected to either PCR analysis or DNA sequence analysis. The PCR product of *redBA/gam* in the wild-type λ EG10 was approximately 2 kb. If a PCR product did not show any discrete alteration on the gel, the mutant was classified as one containing a point mutation with either a base substitution or a frameshift causing no alteration in the size of the gene product. In contrast an absence of visible PCR product was taken as evidence of a mutant with a deletion > 2 kb as a result of losing both *redBA* and *gam* genes. The types of mutations identified from analysis of these mutants are listed in Table 1 and Figure 3. To minimize the possibility that these isolated mutants were spontaneously derived, we

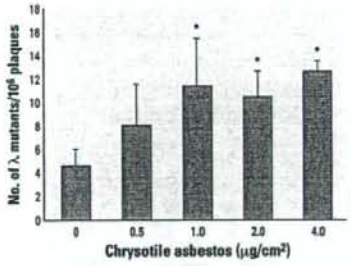

Figure 2. Mutagenic potential of chrysotile asbestos at *redBA* and *gam* loci in transgenic MEF cells. MEF cells, 5×10^5, were treated with graded doses of chrysotile as described in the text. Results were expressed as the total number of confirmed λ mutants divided by the total number of rescued phages. The average number of preexisting mutants per 10^6 plaques used for these experiments was 4.69 ± 1.42. Data were pooled from six independent experiments. Error bars indicate ± SD. *Significantly different at $p < 0.05$.

Table 1. Type of λ-phage mutants at *redBA/gam* loci either of spontaneous origin or induced by chrysotile treatments (1 µg/cm²) determined by multiplex PCR analyses and DNA sequencing.

Groups	Total no. of mutants	No. of mutants with base substitution	No. of mutants with 1-bp deletion	No. of mutants with > 2-bp and < 1-kb deletions	No. of mutants with > 2-kb deletion
Control	93	7 (8%)	68 (73%)	8 (8%)	10 (11%)
Chrysotile	74	5 (7%)	41 (56%)	10 (14%)	17 (23%)

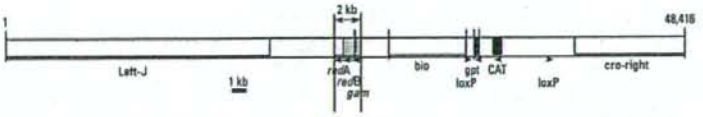

Figure 3. Schematic map of λ EG10 transgene. Abbreviations: bio, genetic marker used in bacteriophage lambda vectors; *CAT*, chloramphenicol acetyltransferase (GenBank accession no. AJ401050; http://www.ncbi.nlm.nih.gov/GenBank/); cro, transcription inhibitor; *gpt*, xanthine phosphoribosyltransferase (GenBank accession no. NP_414773); J, codes for phage tail gene; loxP, locus of X over P1, a site on the bacteriophage P1 consisting of 34 bp; *redA*, *redB*, and *gam*, single copy bacteriophage genes.

selected mutant phages from only the dose of chrysotile that resulted in the highest inductions over background levels. The majority of spontaneous mutants were deletions of various sizes throughout the *red BA/gam* genes (86 of 93 or 92%). Of these deletion mutants, 1 bp deletion made up 68 of 93 or 73%, whereas deletions ranging from 2 bp to 1 kb made up 8 of 93 or 8.6%. Of the spontaneous mutations with deletions 10 of 93 or 11% encompass regions of both the *gam* and *redBA* genes. In contrast, 41 of 74 or 56% and 10 of 74 or 14% of mutants recovered from chrysotile treated cells were single base pair deletion and deletions ranging from 2 bp to 1 kb, respectively. The proportion of mutants induced by chrysotile suffering loss of both the *gam* and *redBA* genes was increased from 10 of 93 or 11% among spontaneous mutants to 17 of 74 or 23% in fiber-treated MEF cells (Table 1).

Deletions > 2 kb contribute to chrysotile-induced mutagenicity. To provide further evidence of the contribution of deletions > 2 kb to the mutagenicity of chrysotile, we compared the frequencies of deletions > 2 kb induced by chrysotile at a dose of 1 μg/cm^2 with those derived spontaneously from control cultures (Table 2). Although the total Spi$^-$ mutant yield in chrysotile-treated cells was 2.4-fold higher than that of controls, the frequency of deletions > 2 kb induced by 1 μg/cm^2 of fibers was 5.2-fold higher than those derived from nontreated control (2.6 vs. 0.5×10^{-6}, $p < 0.005$). The frequency of base substitution and small deletions including single base deletions and deletions < 1 kb formed in fiber-treated MEF cells was only 2-fold higher than those from nontreated cases. These results indicated that the major types of mutations induced by chrysotile were deletions > 2 kb.

Oxyradicals mediated the mutagenicity of chrysotile in transgenic mouse mutation assay system. There is evidence that the genotoxicity/carcinogenicity of asbestos fibers is mediated by reactive oxygen/nitrogen species (Shukla et al. 2003). To demonstrate that oxyradicals mediated the mutagenicity of chrysotile fibers in MEF cells, we exposed MEF cells to either chrysotile for 24 hr in complete medium, or to H_2O_2 in serum free medium for 15 min in the presence or absence of catalase (Figure 4). The relative viability of MEF cells treated with a 1 μg/cm^2 dose of chrysotile was 71%, whereas the relative viability of MEF cells after exposing to 2.9 mM H_2O_2 was 69%. Both chrysotile and H_2O_2 led to significant increases in Spi$^-$ mutant yields in MEF cells. As shown in Figure 4, the mutation yield induced by H_2O_2 treatment was slightly higher than that of chrysotile at equal toxic doses, although the difference was not statistically significant. Furthermore, the mutation yields induced by either chrysotile at a dose of 1 μg/cm^2 or 2.9 mM H_2O_2 were dramatically suppressed in the presence of 5,000 U/mL catalase ($p < 0.05$). Interestingly, the ratio of the mutants with deletions > 2 kb was similar between chrysotile and H_2O_2 in that 20 of 84 or 24% of the mutants induced by 2.9 mM H_2O_2 lost both *redBA* and *gam* genes compared with 17 of 74 or 23% among those induced by a 1-μg/cm^2 dose of chrysotile (Figure 5). The mutant fractions with deletions > 2 kb increased from 0.5 ± 0.16 observed in controls to either 2.6 ± 0.93 or 3.2 ± 1.34 in cells treated with either chrysotile or H_2O_2, respectively. The dose of catalase used here had little effect on the level of cell viability and mutant fraction in control cells. Similarly, heat-inactivated catalase (by boiling for 10 min) had little effect on the mutant fraction in exposed cells.

Induction of γ-H2AX in MEF cells. Among various type of DNA damages, the DSBs in DNA may be the most damaging and genotoxic, which elevate the frequencies of gene translocations, rearrangements, amplifications, and deletions during repair and misrepair of DSBs (Khanna and Jackson 2001). A very early step in the response of mammalian cells to DNA DSBs is the phosphorylation of histone H2AX at serine-139 at the sites of DNA damage. To investigate whether chrysotile induces phosphorylation of H2AX in MEF cells, we exposed cultures to either a 1- or 2-μg/cm^2 dose of chrysotile for 24 hr before being fixed and stained with anti–γ-H2AX antibodies. The expression of phosphorylated H2AX as a function of DNA damage was then analyzed using flow cytometry. The histograms represented the frequency of cell number versus the intensity of the fluorescence signals of γ-H2AX antibody staining [FL1-H (green fluorescence signal received by the photomultiplier tube); Figure 6A]. Even though the number of foci/cell cannot be measured directly by flow cytometry, we found that MEF cells incubated with chrysotile showed an increased staining with anti–γ-H2AX antibodies as detected by immunofluorescence. However, there was no dose-dependent induction of γ-H2AX in MEF cells exposed to either 1 or 2 μg/cm^2 doses of chrysotile (Figure 6B). Concurrent treatment of catalase greatly suppressed the induction of γ-H2AX among treated cells. These results suggest that chrysotile induced DNA damage that triggers a stress response leading to H2AX phosphorylation.

Discussion

Asbestos fiber is an important environmental carcinogen worldwide and remains the primary occupational concern in many developing countries. Although the carcinogenicity of asbestos is well established, the underlying mechanism is not known. We have previously

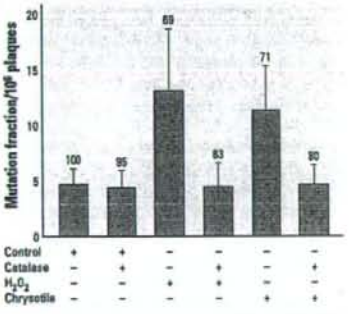

Figure 4. Mutant fractions at *redBA/gam* loci in MEF cells exposed to either chrysotile asbestos at a dose of 1 μg/cm^2 or 2.9 mM H_2O_2 either in the presence (+) or absence (–) of catalase (5,000 U/mL). Results were expressed as the total number of confirmed λ-phage mutants divided by the total number of rescued phages. The average number of preexisting mutants per 10^6 plaques used for these experiments was 4.69 ± 1.42. Numbers above error bars indicate the percentage of relative viability. Data were pooled from three to six independent experiments. Error bars indicate ± SD.

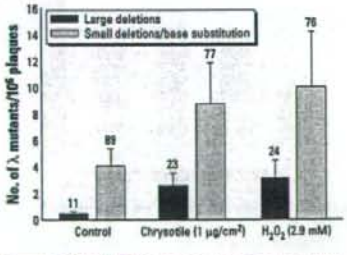

Figure 5. Mutant fractions of λ-phage mutants with specific molecular characteristics in MEF cells exposed to either chrysotile at a concentration of 1 μg/cm^2 or H_2O_2 at a dose of 2.9 mM. Numbers above error bars indicate ratio of mutation type calculated as percentage. Data were pooled from three to six independent experiments. Error bars indicate ± SD.

Table 2. Mutant fractions of deletions involving the *redBA/gam* region and other smaller deletions including single base changes in either nontreated control cells or cells treated with chrysotile fibers (1 μg/cm^2 for 24 hr).

	Control	Asbestos
Total mutant fraction at *redBA/gam* loci	4.69×10^{-6}	11.4×10^{-6}
Large deletions (> 2 kb)		
Mutant fraction	0.5×10^{-6}	2.6×10^{-6}
Increase above the control	1.0	5.2
Small deletions plus single base changes		
Mutant fraction	4.2×10^{-6}	8.8×10^{-6}
Increase above the control	1.0	2.1

demonstrated that asbestos fibers are mutagenic and induce gene/chromosomal mutations in mammalian cells. Similar results have subsequently been reported by others using various *in vitro* and *in vivo* assays that can quantify multilocus deletions (Hei et al. 1992; Lezon-Geyda et al. 1996; Park and Aust 1998). However, it has not been established how asbestos fibers induce such mutational events *in vivo*.

Inhalation studies in Big Blue *lacI* transgenic mice have revealed that there is a 1.96-fold increase in mutation frequencies in lung tissues of crocidolite-exposed mice compared with nonexposed control mice, but no specific mutant spectrum has been identified (Rihn et al. 2000). More recently, mutation induction factors ranging from 1.1 to 3.2 in the omenta have been reported in Big Blue *lacI* transgenic rats injected with crocidolite (Unfried et al. 2002). Intratracheal instillation with amosite results in a 2-fold increase in the mutation frequency in lung DNA in Big Blue *lacI* transgenic rats (Topinka et al. 2004). It should be noted that the *lacI* transgenic system is limited to small sequence alterations between 1 and 20 bp, such as point mutations, small deletions, and insertions. Most genome mutations such as large deletions and insertions, translocations, and aneuploidy cannot be effectively recovered by the *lacI* shuttle vector. Several studies in which mutation frequencies in the *lacI* transgenic system were compared with that in endogenous genes have shown that spontaneous mutation frequencies at reporter genes were dramatically higher than those found at the endogenous *hprt* gene (Skopek et al. 1995; Walker et al. 1999). It is likely that overall mutagenesis induced by asbestos fibers may be underestimated in Big Blue *lacI* mice. As such, it is extremely desirable to establish an efficient system to recover large deletion events induced by asbestos fibers *in vivo*.

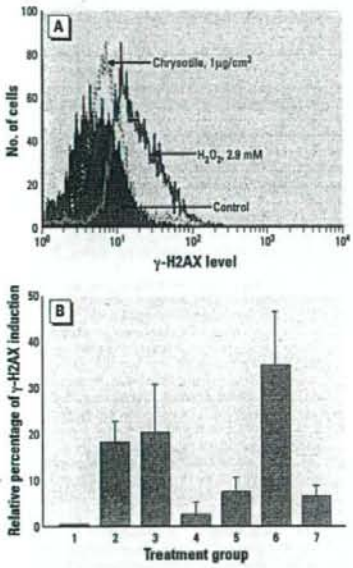

Figure 6. Accumulation of γ-H2AX in MEF cells exposed to either chrysotile for 24 hr in completed medium or H_2O_2 for 15 min in serum-free medium in the presence or absence of catalase. (*A*) Generation of γ-H2AX in cells treated with either chrysotile or H_2O_2 detected by flow cytometry using mouse monoclonal anti–γ-H2AX labeled with FITC. Results are shown using FL1-H. (*B*) Induced γ-H2AX in MEF cells exposed to either chrysotile or H_2O_2 in the presence or absence of catalase. (1) Control; (2) 1 μg/cm² chrysotile; (3) 2 μg/cm² chrysotile; (4) 5,000 U/mL catalase; (5) 1 μg/cm² chrysotile + 5,000 U/mL catalase; (6) 29 mM hydrogen peroxide; (7) 29 mM hydrogen peroxide + 5,000 U/mL catalase. Data were pooled from three independent experiments. Error bars indicate ± SD.

The *gpt* delta transgenic mouse system, established in the laboratory of one of the coauthors provides a unique opportunity to assess the *in vivo* mutagenic potential of mineral fibers (Masumura et al. 2003; Nohmi and Masumura 2004, 2005). The *gpt* delta mice carry tandem repeats of λ EG10 DNA in two units of 40 phage copies each on both arms of chromosome 17, which are retrievable as phage particles by an *in vitro* packaging reaction. The rescued phages are then used to quantify the mutation yield upon exposure to genotoxic agents. In the present study the MEF cells from the transgenic mice were used to both quantify and characterize the deletions induced by graded doses of chrysotile fibers. Our results demonstrated that chrysotiles induced a dose dependent increase in mutant yield at the *gam* and *redBA* loci in MEF cells and that the incidence and types of mutants generated were comparable to those induced by equitoxic doses of H_2O_2.

Among the mutants with deletions ≥ 2 kb that span the *redBA/gam* gene, the mutant fraction induced by treatment with a 1 μg/cm² dose of chrysotiles was 5.2-fold higher than those derived spontaneously. The mutant fraction and the number of mutants with deletions > 2 kb, however, were not elevated by further increase in fiber doses. Although the precise reason for this lack of dose–response relationship is not clear, it is possible that mutated cells were selectively killed or that the λ phages were not effectively recovered *in vitro* at high fiber doses. In addition to large deletions, the small mutational events observed were predominantly single base pair deletions at the *gam* locus in both spontaneous mutants and mutants induced by asbestos (Table 1). There is evidence that deletions in the *gam* gene not only inactivate the *gam* gene but also interfere with the translation of the *redBA* gene, leading to functionally inactivate *gam* and *redBA* genes (Masumura et al. 2003). It should be noted that the maximum size of deletions detectable by the Spi⁻ assay is 9.6 kb. However, deletions extending into regions adjacent to the transgene concatemer are not detected, as two intact cos sites are required for the packaging of a single λ vector. Our present study indicated that the maximum deletion generated by chrysotiles in the *gpt* delta transgenic mutation system were kilobase-sized intrachromosomal deletions, which were much smaller than our previous reports on megabase–sized multilocus deletions generated by asbestos in the human–hamster cells (Hei et al. 1992), largely because of the nature of the model system.

Various *in vitro* and *in vivo* studies have indicated that oxyradicals are one of the key determinants of asbestos-induced mutagenesis and carcinogenesis (Shukla et al. 2003). Among the most biologically active oxyradicals (e.g., superoxide anions ($O_2^{\bullet}$), hydroxyl radical ($^{\bullet}OH$), singlet oxygen ($^1O_2$), and hydroperoxy radical ($HO_2^{\bullet}$), H_2O_2 is relatively long-lived and directly crosses cell membranes by simple diffusion (Root et al. 1975). There is evidence that H_2O_2 not only induces damage to DNA, causing single- and double-strand breaks, base loss, base substitution, and cross-linking, but also causes chromosome and chromatid aberrations (Mondello et al. 2002). Recently, 8-hydroxydeoxyguanosine, an oxidative DNA damage marker, has been detected in Big Blue *lacI* transgenic rats treated with asbestos (Unfried et al. 2002). In an effort to understand the molecular mechanisms involved in the intra-chromosomal deletions induced by chrysotile in the present model, we compared mutation patterns between chrysotile asbestos and ROS. In the absence of serum, H_2O_2 produced predominantly $^{\bullet}OH$ radicals in human fibroblast culture (Weitzman and Graceffa 1984). Our results showed that for chrysotile-induced λ mutants the ratios of mutants with large deletions were similar to those induced by H_2O_2 at equitoxic doses. From a mechanistic point of view, these data suggest that similar mutagenic mechanisms are involved between asbestos fibers and chemically generated ROS. Consistent with this possibility, large mutational events mediated by oxyradicals have been observed in the human–hamster, AS52, and L5178 systems (Fach et al. 2003; Lipinski et al. 2000; Xu et al. 2002).

DSBs are usually regarded as the most deleterious type of DNA damage, induced either by environmental stress, such as irradiation or oxidative stress by the stalling of DNA replication forks (O'Driscoll and Jeggo 2006). Inefficient or inaccurate repair can elevate the frequencies of deletion, amplification, and chromosomal translocation, leading to chromosomal instability and neoplastic transformation. There is evidence that survival

fraction and DSB-repair efficiency are dramatically decreased by chrysotile asbestos in the DNA DSB repair deficient cells as compared with wild-type cells (Okayasu et al. 1999). A very early step in the response of mammalian cells to DNA DSBs is the phosphorylation of histone H2AX at serine 139 at the sites of DNA damage (Lowndes and Toh 2005). Using γ-H2AX as a biomarker for DNA DSBs, our data showed that the accumulation of γ-H2AX was greatly increased by chrysotile treatment in MEF cells, which was inhibited by concurrent treatment with catalase. These findings provided strong corroborating evidence of the DNA damaging effects of chrysotiles through the oxyradical pathway.

Chromosomal rearrangements have been closely associated with the progression and maintenance of cancer (Radford 2004). One of the major difficulties in detecting *in vivo* somatic mutations in chromosomal DNA is the lack of systems capable of identifying and isolating mutated genes with high efficiency. Spi⁻ selection based on deletions extending into or through both the *redBA* and *gam* genes is an efficient mutation assay system for detecting small to kilobase-sized deletions in different cells, organs, and tissues (Nohmi and Masumura 2004). Although during packaging, the individual genes and vectors are segregated from each other and assayed for mutation independently, the target genes in the *gpt* delta system are present in multiple copies in tandem arrays and amount to a potential target of approximately 3.8 Mb. In reality megabase deletions cannot be distinguished from kilobase deletions because of the size limitation of lambda phage to be packaged. Thus, it is likely that the deletions that are induced by asbestos fibers in the present study may include intergenic deletions whose sizes are > 10 kb. As gene mutation, mitotic recombination, chromosome loss, and interstitial deletion largely contribute to the development of malignancy, the establishment of the *gpt* delta transgenic mouse mutation model may provide novel, mechanistic information on asbestos-induced genotoxicity in the future.

Reference

Bernstein DM, Rogers R, Smith P. 2003. The biopersistence of Canadian chrysotile asbestos following inhalation. Inhal Toxicol 15(13):1247–1274.

Coin PG, Roggli VL, Brody AR. 1994. Persistence of long, thin chrysotile asbestos fibers in the lungs of rats. Environ Health Perspect 102(suppl 5):197–199.

Dean SW, Brooks TM, Burlinson B, Mirsalis J, Myhr B, Recio L et al. 1999. Transgenic mouse mutation assay systems can play an important role in regulatory mutagenicity testing in vivo for the detection of site-of-contact mutagens. Mutagenesis 14(1):141–151.

Fach E, Kristovich R, Long JF, Waldman WJ, Dutta PK, Williams MV. 2003. The effect of iron on the biological activities of erionite and mordenite. Environ Int 29(4):451–458.

Gardner MJ, Saracci R. 1989. Effects on health of non-occupational exposure to airborne mineral fibres. IARC Sci Publ 90:375–397.

Gustavsson P, Jakobsson R, Johansson H, Lewin F, Norell S, Rutkvist LE. 1998. Occupational exposures and squamous cell carcinoma of the oral cavity, pharynx, larynx, and oesophagus: a case-control study in Sweden. Occup Environ Med 55(6):393–400.

Hei TK, Piao CQ, He ZY, Vannais D, Waldren CA. 1992. Chrysotile fiber is a strong mutagen in mammalian cells. Cancer Res 52(22):6305–6309.

Hogan B, Beddington R, Constantini F, and Lacy E. 1994. Manipulating the Mouse Embryo, 2nd ed. Cold Spring Harbor, NY: Cold Spring Harbor Laboratory Press.

Horiguchi M, Masumura KI, Ikehata H, Ono T, Kanka Y, Nohmi T. 2001. Molecular nature of ultraviolet B light-induced deletions in the murine epidermis. Cancer Res 61(10):3913–3918.

International Agency for Research on Cancer. 1987. Overall Evaluation of Carcinogenicity: an Updating of IARC Monographs Volumes 1–42. IARC Monogr Eval Carcinog Risks Hum Supplement 7.

Jaurand MC. 1996. Use of in vitro genotoxicity and cell transformation assays to evaluate the potential carcinogenicity of fibres. IARC Sci Publ 140:55–72.

Khanna KK, Jackson SP. 2001. DNA double-strand breaks: signaling, repair and the cancer connection. Nat Genet 27(3): 247–254.

Kjaerheim K, Ulvestad B, Martinsen JI, Andersen A. 2005. Cancer of the gastrointestinal tract and exposure to asbestos in drinking water among lighthouse keepers (Norway). Cancer Causes Control 16(5):583–598.

Kurose A, Tanaka T, Huang X, Halicka HD, Traganos F, Dai W et al. 2005. Assessment of ATM phosphorylation on Ser-1981 induced by DNA topoisomerase I and II inhibitors in relation to Ser-139-histone H2AX phosphorylation, cell cycle phase, and apoptosis. Cytometry A 68(1):1–9.

Lazon-Geyda K, Jaime CM, Godbold JH, Savransky EF, Hope A, Kheiri SA, et al. 1996. Chrysotile asbestos fibers mediate homologous recombination in Rat2 lambda fibroblasts: implications for carcinogenesis. Mutat Res 361(2–3):113–120.

Lipinski P, Drapier JC, Oliveira L, Retmanska H, Sochanowicz B, Kruszewski M. 2000. Intracellular iron status as a hallmark of mammalian cell susceptibility to oxidative stress: a study of L5178Y mouse lymphoma cell lines differentially sensitive to H_2O_2. Blood 95(9):2960–2966.

Lowndes NF, Toh GW. 2005. DNA repair: the importance of phosphorylating histone H2AX. Curr Biol 15(3):R99–R102.

Masumura K, Totsuka Y, Wakabeyashi K, Nohmi T. 2003. Potent genotoxicity of aminophenylnorharman, formed from non-mutagenic norharman and aniline, in the liver of *gpt* delta transgenic mouse. Carcinogenesis 24(12):1985–1993.

Miller A. 2005. Mesothelioma in household members of asbestos-exposed workers: 32 United States cases since 1990. Am J Ind Med 47(5):458–462.

Mondello C, Guasconi V, Giulotto E, Nuzzo F. 2002. Gamma-ray and H_2O_2 induction of gene amplification in hamster cells deficient in DNA double strand break repair. DNA Repair (Amst) 1(6):483–493.

Nohmi T, Katoh M, Suzuki H, Matsui M, Yamada M, Watanabe M, et al. 1996. A new transgenic mouse mutagenesis test system using Spi⁻ and 6-thioguanine selections. Environ Mol Mutagen 28(4):465–470.

Nohmi T, Masumura K. 2005. Molecular nature of intrachromosomal deletions and base substitutions induced by environmental mutagens. Environ Mol Mutagen 45(2–3):150–161.

Nohmi T, Masumura KI. 2004. *Gpt* delta transgenic mouse: a novel approach for molecular dissection of deletion mutations in vivo. Adv Biophys 38:97–121.

O'Driscoll M, Jeggo PA. 2006. The role of double-strand break repair—insights from human genetics. Nat Rev Genet 7(1): 45–54.

Okayasu R, Takahashi S, Yamada S, Hei TK, Ullrich RL. 1999. Asbestos and DNA double strand breaks. Cancer Res 59(2): 298–300.

Pan XL, Day HW, Wang W, Beckett LA, Schenker MB. 2005. Residential proximity to naturally occurring asbestos and mesothelioma risk in California. Am J Respir Crit Care Med 172:1019–1025.

Park SH, Aust AE. 1998. Participation of iron and nitric oxide in the mutagenicity of asbestos in hgprt⁻, gpt⁺ Chinese hamster V79 cells. Cancer Res 58(6):1144–1148.

Poser I, Rahman Q, Lohani M, Yadav S, Becker HH, Weiss DG et al. 2004. Modulation of genotoxic effects in asbestos-exposed primary human mesothelial cells by radical scavengers, metal chelators and a glutathione precursor. Mutat Res 559(1–2): 19–27.

Radford IR. 2004. Chromosomal rearrangement as the basis for human tumourigenesis. Int J Radiat Biol 80(8):543–557.

Rihn B, Coulais C, Kauffer E, Bottin MC, Martin P, Yvon F, et al. 2000. Inhaled crocidolite mutagenicity in lung DNA. Environ Health Perspect 108:341–346.

Rom WN, Hammar SP, Rusch V, Dodson R, Hoffman S. 2001. Malignant mesothelioma from neighborhood exposure to anthophyllite asbestos. Am J Ind Med 40(2):211–214.

Root RK, Metcalf J, Oshino N, Chance B. 1975. H_2O_2 release from human granulocytes during phagocytosis. I. Documentation, quantitation, and some regulating factors. J Clin Invest 55(5): 945–955.

Scudiero DA, Shoemaker RH, Paull KD, Monks A, Tierney S, Nofziger TH, et al. 1988. Evaluation of soluble tetrazolium/formazan assay for cell growth and drug sensitivity in culture using human and other tumor cell lines. Cancer Res 48:4827–4833.

Shibata A, Kamada N, Masumura K, Nohmi T, Kobayashi S, Teraoka H, et al. 2005. Parp-1 deficiency causes an increase of deletion mutations and insertions/rearrangements *in vivo* after treatment with an alkylating agent. Oncogene 24(8): 1328–1337.

Shukla A, Gulumian M, Hei TK, Kamp D, Rahman Q, Mossman BT. 2003. Multiple roles of oxidants in the pathogenesis of asbestos-induced diseases. Free Radic Biol Med 34(9): 1117–1129.

Skopek TR, Kort KL, Marino DR. 1995. Relative sensitivity of the endogenous *hprt* gene and *lacI* transgene in ENU-treated Big Blue B6C3F$_1$ mice. Environ Mol Mutagen 26(1):9–15.

Timbrell V. 1970. Characteristics of the International Union Against Cancer Standard Reference Samples of Asbestos. In: Pneumoconiosis, Proceedings of the International Conference, April 1969, Johannesburg, South Africa (Shapiro HA, ed). Cape Town, South Africa:Oxford University Press, 28–36.

Topinka J, Loli P, Georgiadis P, Dusinska M, Hurbankova M, Kovacikova Z, et al. 2004. Mutagenesis by asbestos in the lung of lambda-lacI transgenic rats. Mutat Res 553(1–2):67–78.

Unfried K, Schurkes C, Abel J. 2002. Distinct spectrum of mutations induced by crocidolite asbestos: clue for 8-hydroxydeoxyguanosine-dependent mutagenesis *in vivo*. Cancer Res 62(1):99–104.

Walker VE, Andrews JL, Upton PB, Skopek TR, deBoer JG, Walker DM, et al. 1999. Detection of cyclophosphamide-induced mutations at the Hprt but not the lacI locus in splenic lymphocytes of exposed mice. Environ Mol Mutagen 34(2–3): 167–181.

Weitzman SA, Graceffa P. 1984. Asbestos catalyzes hydroxyl and superoxide radical generation form H_2O_2. Arch Biochem Biophys 228:373–376.

Xu A, Zhou H, Yu DZ, Hei TK. 2002. Mechanisms of the genotoxicity of crocidolite asbestos in mammalian cells: implication from mutation patterns induced by reactive oxygen species. Environ Health Perspect 110:1003–1008.

DNA REPAIR 7 (2008) 497–506

available at www.sciencedirect.com

ScienceDirect

journal homepage: www.elsevier.com/locate/dnarepair

Specificity of mutations induced by incorporation of oxidized dNTPs into DNA by human DNA polymerase η

Katsuhiko Hidaka[a,b], *Masami Yamada*[a], *Hiroyuki Kamiya*[c], *Chikahide Masutani*[d], *Hideyoshi Harashima*[c], *Fumio Hanaoka*[d], *Takehiko Nohmi*[a,*]

[a] *Division of Genetics and Mutagenesis, National Institute of Health Sciences, 1-18-1 Kamiyoga, Setagaya-ku, Tokyo 158-8501, Japan*
[b] *Graduate School of Global Environmental Studies, Kyoto University, Yoshida-honmachi, Sakyo-ku, Kyoto 606-8501, Japan*
[c] *Faculty of Pharmaceutical Sciences, Hokkaido University, Kita-12, Nishi-6, Kita-ku, Sapporo, Hokkaido 060-0812, Japan*
[d] *Graduate School of Frontier Biosciences, Osaka University and SORST, JST, 1-3 Yamadaoka, Suita, Osaka 565-0871, Japan*

ARTICLE INFO

Article history:
Received 8 August 2007
Received in revised form
9 December 2007
Accepted 11 December 2007
Published on line 31 January 2008

Keywords:
Oxidative mutagenesis
Nucleotide pool
8-Hydroxy-dGTP
2-Hydroxy-dATP
Human DNA polymerase η

ABSTRACT

Aberrant oxidation is a property of many tumor cells. Oxidation of DNA precursors, i.e., deoxynucleotide triphosphates (dNTPs), as well as DNA is a major cause of genome instability. Here, we report that human DNA polymerase η (h Polη) incorporates oxidized dNTPs, i.e., 2-hydroxy-2′-deoxyadenosine 5′-triphosphate (2-OH-dATP) and 8-hydroxy-2′-deoxyguanosine 5′-triphosphate (8-OH-dGTP), into DNA in an erroneous and efficient manner, thereby inducing various types of mutations during in vitro gap-filling DNA synthesis. When 2-OH-dATP was present at a concentration equal to those of the four normal dNTPs in the reaction mixture, DNA synthesis by h Polη enhanced the frequency of G-to-T transversions eight-fold higher than that of the transversions in control where only the normal dNTPs were present. When 8-OH-dGTP was present at an equimolar concentration to the normal dNTPs, it enhanced the frequency of A-to-C transversions 17-fold higher than the control. It also increased the frequency of C-to-A transversions about two-fold. These results suggest that h Polη incorporates 2-OH-dATP opposite template G and incorporates 8-OH-dGTP opposite template A and slightly opposite template C during DNA synthesis. Besides base substitutions, h Polη enhanced the frequency of single-base frameshifts and deletions with the size of more than 100 base pairs when 8-OH-dGTP was present in the reaction mixture. Since h Polη is present in replication foci even without exogenous DNA damage, we suggest that h Polη may be involved in induction of various types of mutations through the erroneous and efficient incorporation of oxidized dNTPs into DNA in human cells.

1. Introduction

Reactive oxygen species (ROS) are produced by normal cellular respiration, cell injury or by exposure to environmental carcinogens and radiation. ROS generate a variety of altered purines and pyrimidines in DNA [1,2], thereby playing important roles in mutagenesis, carcinogenesis and aging [3,4]. It should be emphasized, however, that oxidized bases in DNA are introduced not only by direct oxidation of DNA but also by incorporation of oxidized deoxynucleotide triphosphates (dNTPs) into DNA by DNA polymerases [5–7]. Indeed, the frequency of A-to-C transversion mutations increases more

* *Corresponding author.* Tel.: +81 3 3700 9873; fax: +81 3 3707 6950.
E-mail address: nohmi@nihs.go.jp (T. Nohmi).
1568-7864/$ – see front matter © 2007 Elsevier B.V. All rights reserved.
doi:10.1016/j.dnarep.2007.12.005

than a 1000-fold over the wild-type level in *Escherichia coli mutT* mutants, which are deficient in the ability to hydrolyze oxidized dGTP, i.e., 7,8-dihydro-8-oxo-dGTP (8-hydroxy-dGTP, 8-OH-dGTP) [8,9]. 8-OH-dGTP leads to A-to-C mutations when it is incorporated opposite adenine (A) in the template DNA because the incorporated 8-OH-G in DNA can pair with incoming dCMP in the next round of DNA replication [6,10]. The high spontaneous A:T-to-C:G mutations in the *mutT* strain are almost completely suppressed when the *mutT* cells are cultured in anaerobic conditions, indicating the essential role of oxygen in the mutagenesis [11]. Another oxidized nucleotide, i.e., 1,2-dihydro-2-oxo-dATP (2-hydroxy-dATP, 2-OH-dATP), can induce G-to-T transversions when it is incorporated opposite guanine (G) in the template [12,13]. The sanitizing enzyme, i.e., Orf135, in *E. coli* degrades 2-OH-dATP, and G:C-to-T:A mutations occur in the *Orf135*-deficient strain more frequently than in the wild-type strain [14,15].

Oxidized dNTPs also cause genome instability in mammalian cells. Spontaneous tumorigenesis in the mice deficient in *Mth1*, a mammalian counterpart of *mutT*, is much enhanced in lung, liver and stomach, and the MTH1 protein hydrolyzes both 8-OH-dGTP and 2-OH-dATP [16,17]. Recent studies with mismatch repair (MMR)-defective cells suggest that the majority of mutations in human cells that are deficient in MMR functions do not arise from spontaneous replication errors, but from the incorporation of oxidized dNTPs [18,19]. Thus, it is of great interest in the mechanisms as to how these oxidized dNTPs induce genome instability and oxidative mutagenesis, which lead to carcinogenesis.

The roles of oxidized dNTPs in mutagenesis have been questioned, however, because oxidized dNTPs are in general poor substrates for DNA polymerases (Pols) [20]. 8-OH-dGTP is poorly incorporated into DNA by Pol δ, T7 Pol exo$^-$, HIV reverse transcriptase, *E. coli* Pol II and Klenow exo$^-$ [21,22]. An exception may be human Pol β, which incorporates 8-OH-dGTP into DNA with an efficiency of 10–20% of normal dGTP incorporation and favors to incorporate it opposite template A [23]. 2-OH-dATP is also a poor substrate for mammalian Pols. The efficiencies of incorporation of 2-OH-dATP opposite template T and C by Pol α are more than 100-fold and 1000-fold, respectively, lower than those of incorporation of normal dATP and dGTP [24].

The Y-family DNA Pols are recently recognized Pols that comprise proteins from different species, including members of eukarya, archaea and bacteria [25]. The most distinct feature of this family of enzymes is their ability to bypass various lesions, such as ultraviolet light photoproducts, in template DNA [26–28]. Some bypass reactions, i.e., translesion DNA synthesis (TLS), catalyzed by these enzymes are error prone while others are error free [29]. Thus, this family of Pols seems to be involved in mutagenesis and DNA-damage tolerance [30]. Interestingly, some of Y-family Pols have been shown to incorporate oxidized dNTPs into DNA in an efficient and erróneous manner. In humans, Polη (h Polη) incorporates 8-OH-dGTP opposite template A at almost the same efficiency as incorporation of normal dTTP, and incorporates 2-OH-dATP opposite template T, G and C at substantial rates [31]. Archaeal Y-family Pols of *Sulfolobus* sp. and a Y-family Pol of *E. coli*, i.e., DNA Pol IV (DinB), almost exclusively incorporate 8-OH-dGTP opposite template A, and 2-OH-dATP opposite template G and thymine (T) [32,33]. In fact, both Y-family DNA Pols of *E. coli*, i.e., Pol IV and Pol V (UmuD'C), are shown to be involved in oxidative mutagenesis in *sod/fur* mutants where the mutator effects are caused by oxidation of dNTPs instead of DNA [33]. Collectively, these results suggest that some of Y-family Pols may be involved in mutagenesis through the erroneous incorporation of oxidized dNTPs into DNA.

In this study, we characterized mutations induced by incorporation of 8-OH-dGTP or 2-OH-dATP into DNA by h Polη using in vitro gap-filling assay with M13mp2 phage DNA [34]. The assay allows us to analyze not only base substitutions but also frameshifts and deletions, which are generated during DNA synthesis to fill in a gap of 407 base pairs (bps) in M13 DNA. We show here that h Polη incorporates 8-OH-dGTP into DNA, thereby inducing single-base frameshifts and large deletions as well as base substitutions including A-to-C transversions. Addition of a quite small amount of 8-OH-dGTP, i.e., 1/1000 amount of the four normal dNTPs, into the reaction mixture enhanced mutagenesis significantly. h Polη also incorporates 2-OH-dATP opposite template G, thereby inducing G-to-T transversions. Because h Polη is present in replication factories in cells not deliberately exposed to DNA damaging agents [35,36], we suggest that h Polη may be involved in a variety of oxidative mutagenesis through the incorrect and efficient incorporation of oxidized dNTPs during DNA synthesis in human cells.

2. Materials and methods

2.1. Materials

h Polη was prepared as described [37]. 8-OH-dGTP was purchased from Trilink Bio Tech, and 2-OH-dATP was purified as described [24]. Normal dNTP mixture was purchased from TAKARA Bio Inc. (Kyoto, Japan). Restriction enzyme *Pvu*II was purchased from New England Biolabs (Massachusetts, USA). Oligonucleotides were from Japan Bio Services Co., Ltd. (Saitama, Japan).

The *E. coli* strain MC1061 and CSH50 were used for electroporation and phage growth, respectively, and M13mp2 bacteriophage was for construction of gapped DNA substrate [34]. These are gifts from Dr. Thomas A. Kunkel, National Institute of Environmental Health Sciences (NIEHS), USA.

2.2. Preparation of gapped M13 DNA and gap-filling reactions by h Polη

The gapped M13mp2 DNA was constructed in way that a 407-bp single-stranded gap contains the *lacZ* α-complementation target sequence [34]. As the first transcribed nucleotide of the *lacZ* gene is numbered +1, the single-stranded gap was numbered nucleotide +191 to −216 and the 5′ end of the *lacZ* gene-84.

Reaction mixtures (15 μL) contained 40 mM tris–HCl (pH 8.0), 10 mM DTT, 3.75 μg BSA, 60 mM KCl, 2.5% glycerol, 10 mM $MgCl_2$, 1.4 nM gapped M13mp2 DNA, 72 nM h Polη and 200 μM of the four normal dNTPs. An equimolar concentration (200 μM) of oxidized dNTP, i.e., 2-OH-dATP or 8-OH-dGTP, was added to the reaction mixtures, if necessary. In this study, we

Table 1 – Mutant frequency induced by oxidized dNTPs

Condition	Total plaques counted	Mutant plaques counted	Mutant frequency	Mean ± S.D.
Control	5308	2076	0.39	0.40 ± 0.01
	6382	2580	0.40	
	8207	3443	0.41	
Plus 2-OH-dATP	3900	1180	0.30	0.36 ± 0.05
	1767	706	0.40	
	8100	3020	0.37	
Plus 8-OH-dGTP	1200	1012	0.84	0.85 ± 0.01*
	950	819	0.86	
	1392	1195	0.86	

The four normal dNTPs (200 μM) were included in the reaction mixture containing h Polη (72 nM). In plus 2-OH-dATP and plus 8-OH-dGTP conditions, 200 μM of 2-OH-dATP or 8-OH-dGTP, respectively, was additionally included in the reaction mixture. Asterisk indicates a significant difference ($P < 0.05$ versus control).

refer to these conditions as "plus 2-OH-dATP" or "plus 8-OH-dGTP" conditions, respectively. To examine the mutagenicity of 8-OH-dGTP at lower concentrations, reactions were conducted with lower concentrations (0.02, 0.2, 2.0 and 20 μM) of 8-OH-dGTP in the presence of the four normal dNTPs (200 μM) and h Polη (72 nM). The gap-filling reactions were carried out at 37 °C for 2 h and terminated by adding EDTA to the final concentration of 15 mM. Completion of the gap-filling reaction was confirmed by agarose gel electrophoresis of the reaction products [34]. Mutagenesis experiments were conducted only when the completion of the reactions was confirmed.

2.3. *Gap-filling assay and determination of mutant frequencies (MFs)*

The gap-filled DNAs were introduced into *E. coli* MC1061 by electroporation at 1.8 kV with Micro pulser set (Bio-Rad) and proliferated in *E. coli* strain CSH50 for α-complementation of β-galactosidase as described [34]. MC1061 was used for electroporation due to its higher efficiency of DNA incorporation than CSH50. Wild-type plaques were dark blue while mutant plaques were light blue or colorless. The experiments were repeated three times in each condition, i.e., control, plus 2-OH-dATP and plus 8-OH-dGTP. MFs were calculated by dividing the numbers of mutant plaques by the total numbers of plaques, and the mean ± standard deviation (S.D.) of three experiments were calculated.

2.4. *Determination of numbers of mutations per DNA molecule*

To determine the number of mutations per DNA molecule, we isolated DNA from independent *lacZ* mutants and sequenced nucleotides +191 through −84 using an ABI PRISM Dye Terminator Cycle Sequencing Kit and an ABI PRISM 310 Genetic Analyzer (Applied Biosystems Japan, Tokyo). When deletions were detected beyond position −84, we expanded the sequence analysis through −216 to determine the length and start/end points of the deletions. We then calculated the average numbers of each type of mutations per DNA molecule ± S.D. of three experiments. In the calculation, we estimated the numbers of DNA molecules by dividing the numbers of sequenced mutant plaques by the MF. In other words, the numbers of mutations in sequenced mutant plaques was divided by the total number of mutant and corresponding wild-type plaques. The statistical significance of the results was examined by the Student's *t*-test.

3. Results

3.1. *Mutations induced by incorporation of oxidized dNTPs into DNA by h Polη*

We began this study by determining the MFs in the *lacZ* gene when the gap of M13mp2 DNA was filled by h Polη with or without oxidized dNTPs. In agreement with the previous report [38], the MF was high of 40% even in the control condition where only the four normal dNTPs were present in the reaction mixture (Table 1). The MF in plus 2-OH-dATP condition was similar to that in the control. In contrast, inclusion of 8-OH-dGTP at a concentration equal to that of normal dNTPs yielded about two-fold increase in MF, i.e., 85% ($P = 0.00015$).

3.2. *Spectra of mutations induced by 2-OH-dATP and 8-OH-dGTP*

To determine what types of mutations were induced by incorporation of oxidized dNTPs, we isolated DNA from 33, 34 and 67 mutant plaques from triplicate experiments of control, plus 2-OH-dATP and plus 8-OH-dGTP conditions, respectively, and sequenced them in the nucleotides +191 through −84. The mutants contained multiple sequence changes per DNA molecule, consistent with the colorless phenotype of most of the plaques (Table 2). Even in the control reactions, the mutants had more than five mutations per molecules (5.70 ± 0.74) and about 85% of the mutations were base substitutions (398/457 mutations, Supplement Table 1). Of the base substitutions, more than 90% were single-base substitutions (362/398) and tandem-base substitutions were rare (18/398). Similar distribution of mutations was observed in plus 2-OH-dATP condition. The mutants contained more than five mutations per DNA molecule (5.70 ± 1.57) and more than 90% of the mutations were base substitutions (485/540 mutations). About 90% of the base substitutions were single-base substitutions (423/485) and tandem-base

Table 2 – Classification of mutations induced by oxidized dNTPs

Mutation	Number of mutations per DNA molecule[a]		
	Control	Plus 2-OH-dATP	Plus 8-OH-dGTP
Base substitution	4.91 ± 0.67	5.12 ± 1.43	16.49 ± 3.92[b]
Deletion	0.50 ± 0.04	0.37 ± 0.10	1.18 ± 0.27[b]
Addition	0.17 ± 0.05	0.14 ± 0.04	0.44 ± 0.26
Complex	0.11 ± 0.07	0.07 ± 0.04	0.25 ± 0.11
Total mutation	5.70 ± 0.74	5.70 ± 1.57	18.35 ± 3.84[b]

[a] The mean ± S.D. of three experiments. The number of DNA molecule was estimated by dividing the number of sequenced mutant plaques by the MF shown in Table 1.
[b] A significant difference with $P < 0.05$ versus control.

substitutions were rare (30/485). However, the percentage of transversions (48% = 233/485) was slightly higher compared to that of transversions in the control (41% = 163/398). In contrast, the number of base substitutions per DNA was about three-fold higher in plus 8-OH-dGTP condition than in the control (16.49 ± 3.92 versus 4.91 ± 0.67, $P = 0.040$). Besides base substitutions, the number of deletions per DNA molecule also increased compared to the control (1.18 ± 0.27 versus 0.50 ± 0.04, $P = 0.041$).

3.2.1. *Base substitutions induced by 2-OH-dATP and 8-OH-dGTP*

To examine what types of base substitutions were induced in plus 2-OH-dATP and plus 8-OH-dGTP conditions, we compared the numbers of specific base substitution mutations per DNA molecule (Fig. 1, Supplement Table 2). In plus 2-OH-dATP condition, the number of G-to-T transversions increased about eight-fold compared to the control (0.79 ± 0.23 versus 0.10 ± 0.08, $P = 0.031$). No other types of base substitutions were increased significantly. In plus 8-OH-dGTP condition, the number of A-to-C transversions per DNA increased 17-fold over the control (8.52 ± 2.20 versus 0.50 ± 0.18, $P = 0.022$). The number of transitions of T-to-C also increased about two-fold (4.26 ± 1.30 versus 2.03 ± 0.35, $P = 0.13$), but the increase was not statistically significant because of the high T-to-C transitions in the control (Fig. 1, Supplement Table 2) [39]. Instead, the number of C-to-A transversions increased significantly although the numbers of C-to-A mutations per DNA were relatively low (0.21 ± 0.03 versus 0.11 ± 0.03, $P = 0.013$). No other base substitutions increased significantly in plus 8-OH-dGTP condition. Since the frequencies of base substitutions were high even in the control, no obvious hotspot sequences were identified in plus 2-OH-dATP and plus 8-OH-dGTP conditions (Supplement Fig. 1).

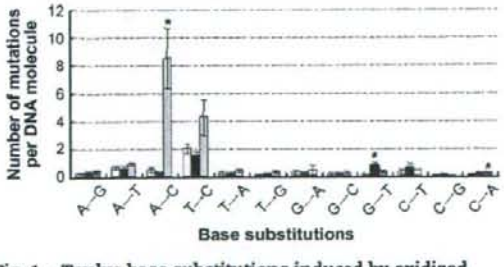

Fig. 1 – Twelve base substitutions induced by oxidized dNTPs. Frequencies of base substitutions are represented as numbers of base substitutions per DNA molecule. Asterisks indicate a significant difference versus control with $P < 0.05$. Each group of bars consists of the results from control (in white), a plus 8-OH-dGTP condition (in gray), and a plus 2-OH-dATP condition (in black). Exact values are presented in Supplement Table 2.

Table 3 – Classification of deletions induced by 8-OH-dGTP

Deletion		Number of mutations per DNA molecule[a]	
		Control	Plus 8-OH-dGTP
One base deletion	ΔA	0.16 ± 0.09	0.10 ± 0.12
	ΔG	0.05 ± 0.06	0.14 ± 0.12
	ΔC	0.02 ± 0.04	0.19 ± 0.05[b]
	ΔT	0.06 ± 0.04	0.33 ± 0.05[b]
	Total	0.29 ± 0.04	0.76[b] ± 0.16
2-99 bases deletion		0.23 ± 0.04	0.30 ± 0.08
>100 bases deletion		<0.01	0.13[b] ± 0.09

[a] The mean ± S.D. of three experiments. The number of DNA molecule was estimated by dividing the number of sequenced mutant plaques by the MF shown in Table 1.
[b] A significant increase with $P < 0.05$ versus control.

3.2.2. *Single-base frameshifts and large deletions induced by 8-OH-dGTP*

To examine what types of deletions were induced in plus 8-OH-dGTP condition, we compared the numbers of deletion mutations per DNA molecule between control and plus 8-OH-dGTP conditions (Table 3, Fig. 2). The numbers of single-base deletions at template C and T increased more than eight-fold and five-fold, respectively, compared to the control condition (0.19 ± 0.05 versus 0.02 ± 0.04 for ΔC $P = 0.031$, and 0.33 ± 0.05 versus 0.06 ± 0.04 for ΔT $P = 0.030$). When we looked for characteristic sequences around the deleted bases, we noticed that G was disfavored at 5′-side of the deleted bases. Only five out of 62 single-base deletions occurred in a sequence of 5′-GX-3′ where X represents the deleted bases, i.e., A, T, G or C. Among other three bases, C was slightly favored at the 5′-side (27/62) while A and T were present evenly (14/62 and 16/62). Besides one-base deletions, large deletions with the size of more than 100 bps increased more than 10-fold compared to the controls

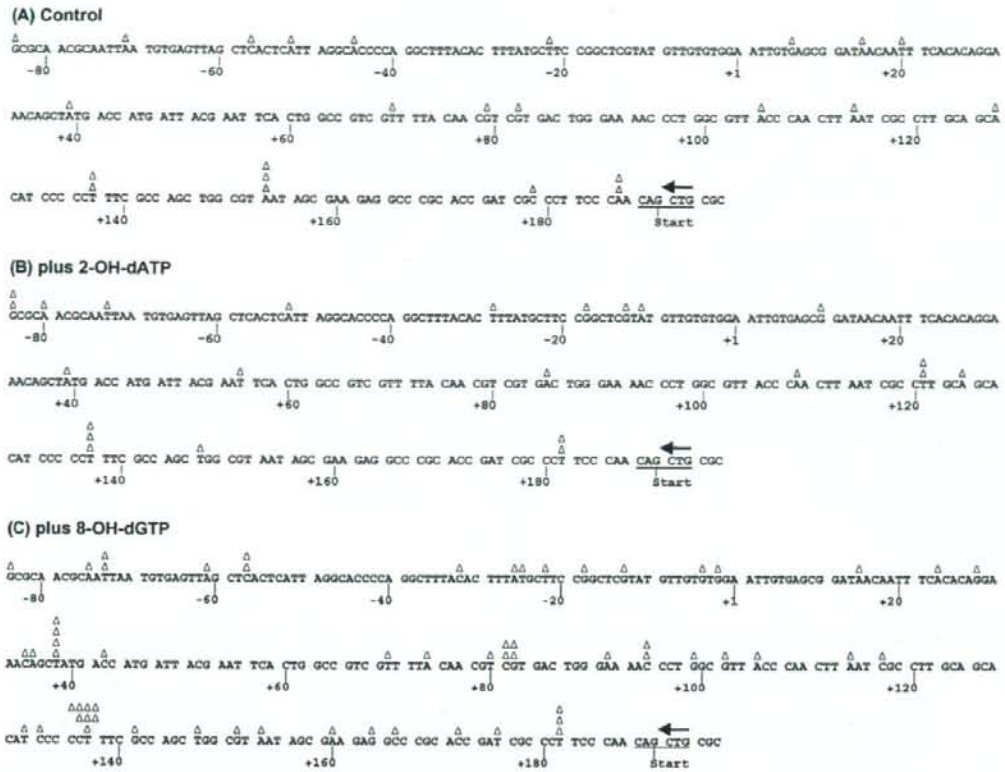

Fig. 2 – Spectra of one-base deletions by h Polη. (A) Control, (B) plus 2-OH-dATP and (C) plus 8-OH-dGTP conditions. One-base deletions are shown as triangles above the template sequence of nucleotide −84 to +194 of the *lacZ* gene in M13mp2 DNA. Nucleotide +1 is the first transcribed nucleotide. DNA synthesis starts at nucleotide +191 and the direction is shown with an arrow.

(0.13 ± 0.09 versus < 0.012). In fact, there were no such large deletions in the mutant plaques from the control and only one in plus 2-OH-dATP condition. The large deletions in plus 8-OH-dGTP mostly occurred between two GC-rich regions, i.e., one-region nucleotides −150 and −140 and the other from +165 to +169 in the *lacZ* gene (Fig. 3).

3.3. *Significant increase in MFs at low concentrations of 8-OH-dGTP*

To examine whether low concentrations of 8-OH-dGTP can induce mutations under the experimental conditions, we lowered the concentrations of 8-OH-dGTP from 200 to 0.02 μM in the reaction mixture where the concentrations of the four normal dNTPs were hold at 200 μM (Fig. 4, Supplement Table 3). The MFs were 0.802 ± 0.022 at 200 μM, 0.565 ± 0.020 at 20 μM, 0.406 ± 0.022 at 2 μM, 0.391 ± 0.008 at 0.2 μM and 0.352 ± 0.008 at 0.02 μM. Statistically significant increases in MFs over the concurrent control MF, i.e., 0.350 ± 0.004, were observed at concentrations of 200, 20, 2 and 0.2 μM of 8-OH-dGTP but not at a concentration of 0.02 μM. To further analyze the mutations at low concentrations of 8-OH-dGTP, we conducted sequence analysis of the mutants and calculated the specific MFs of A-to-C mutations per DNA molecule. The specific MFs were 8.83 ± 0.99 at 200 μM, 0.51 ± 0.20 at 2 μM, 0.43 ± 0.08 at 0.2 μM, 0.50 ± 0.19 at 0.02 μM and 0.35 ± 0.15 at 0 μM (Supplement Table 4).

4. Discussion

Although h Polη was initially recognized as an error-free bypass Pol across a *cis-syn* thymine–thymine dimer in DNA [26,27], recent evidence suggests that it plays roles in several important DNA transactions besides TLS [40]. Polη may be involved in homologous recombination by interacting with RAD51 [41,42] and may participate in somatic hypermutation of immunoglobulin genes [43]. In addition, Polη is co-localized with replication factories in cells not deliberately exposed to DNA damaging agents [35,36]. Thus, it may constitutively gain access to the genomic DNA and contribute to mutagenesis and/or damage avoidance even without external DNA damage. Interestingly, both Y-family DNA Pols in *E. coli*, i.e., Pol IV (DinB) and Pol V (UmuD'C), have been shown to partici-

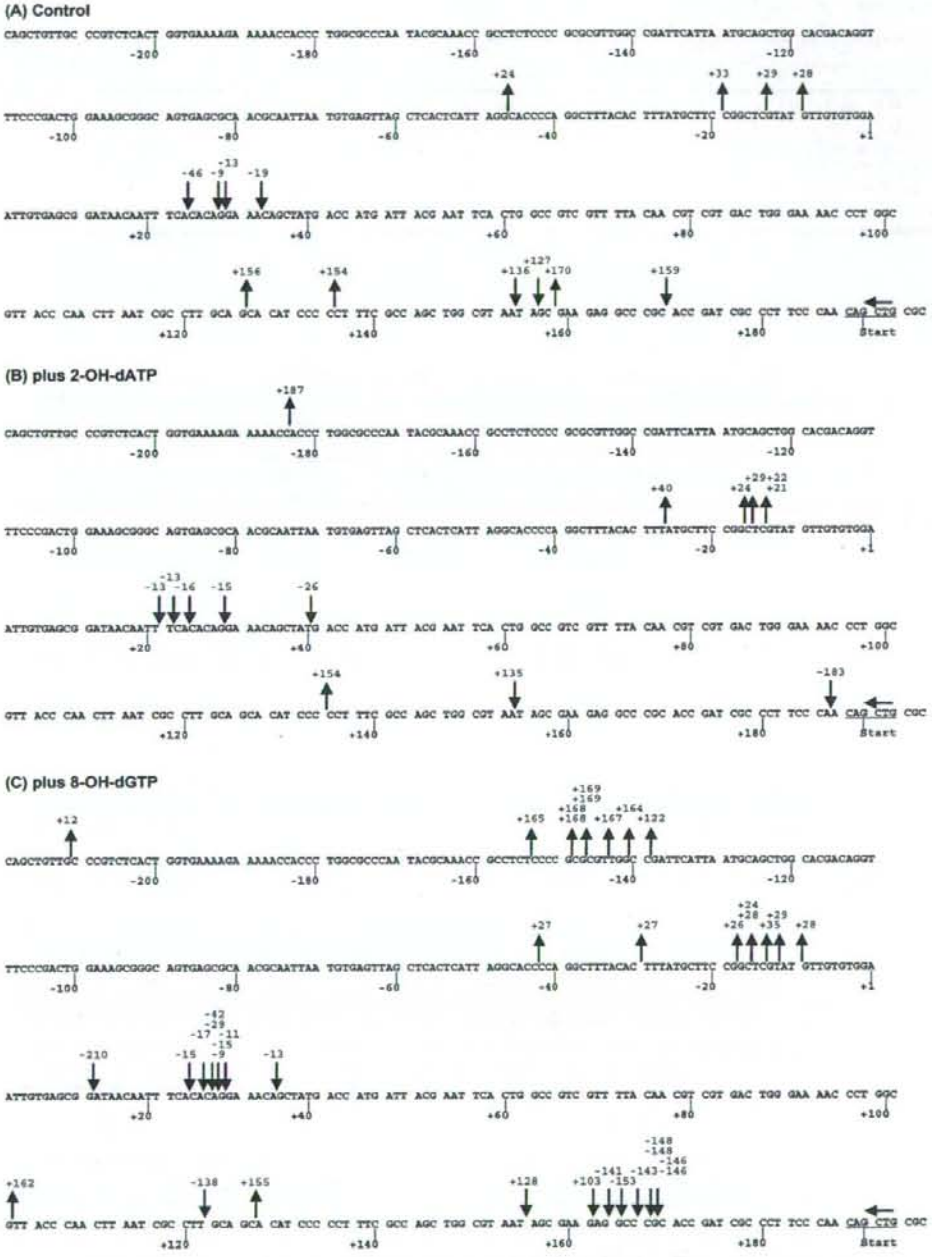

Fig. 3 – Spectra of deletions with the size of more than 10 bps by h Polη. (A) Control, (B) plus 200 μM of 2-OH-dATP and (C) plus 200 μM of 8-OH-dGTP conditions. Each deletion is defined by two arrows; one point down and the other point up. Each arrow is associated with a number indicating the nucleotide position at which the other endpoint for that deletion is located, and each arrow indicates the border between a deleted base and an undeleted base. Nucleotide +1 is the first transcribed nucleotide of the *lacZ* gene in M13mp2 DNA. DNA synthesis starts at nucleotide +191 marked with an arrow, which indicates the direction of DNA synthesis.

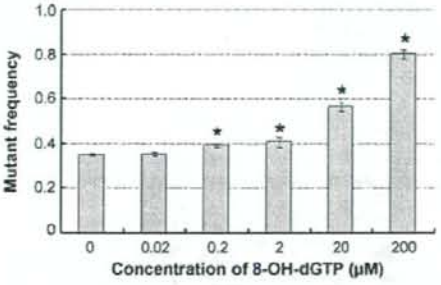

Fig. 4 – Mutant frequencies by h Polη in the presence of various concentrations of 8-OH-dGTP. Asterisks indicate a significant difference versus control, that is, the reaction only with the four normal dNTPs ($P < 0.05$). Exact values are presented in Supplement Table 3.

pate in mutagenesis through the erroneous incorporation of oxidized dNTPs into DNA when oxidation of the nucleotide pool is increased by *sod/fur* mutations [33]. h Polη and the *E. coli* Y-family Pols are involved in the chromosome replication when the cells are treated with hydroxyurea, which does not induce DNA damage but depletes the nucleotide pool [44,45]. h Polη can compete with replicative Pols during in vitro DNA replication [46]. We envisage, therefore, that h Polη might be involved in mutagenesis through misincorporation of oxidized dNTPs when the nucleotide pool is heavily oxidized. In fact, Kamiya et al. observed that knockdown of the expression of h Polη reduced the mutagenicity of 8-OH-dGTP incorporated into human cells (Ph.D. thesis of Dr. K. Satou in Hokkaido University, 2007).

To better understand the roles of h Polη in oxidative mutagenesis, we characterized the mutations induced by incorporation of 2-OH-dATP and 8-OH-dGTP into DNA by h Polη without lesions in template DNA in vitro, and compared the characteristic mutations to those observed in oxidative mutagenesis in mouse and human cells. When 2-OH-dATP was present at an equimolar concentration to the four normal dNTPs during DNA synthesis, incorporation of 2-OH-dATP by h Polη enhanced G-to-T transversions about eight-fold compared to the control where only the normal dNTPs were present (Fig. 1, Supplement Table 2). Because G-to-T transversions are rare, i.e., less than 2% of total mutations in control and plus 2-OH-dATP conditions, the total MF and the numbers of total base substitutions per DNA molecule were not enhanced by addition of 2-OH-dATP in the reaction mixture (Tables 1 and 2). Nevertheless, the significant increase in the frequency of G-to-T transversions in plus 2-OH-dATP condition suggests that h Polη misincorporates 2-OH-dATP opposite template G during the gap-filling reactions in vitro (Fig. 5A). This is consistent with the results of the kinetics analysis that h Polη tends to incorporate 2-OH-dATP opposite T, G and C in this order [31].

Intriguingly, Russo et al. [19] report that over-expression of hMTH1, which hydrolyzes both 2-OH-dATP and 8-OH-dGTP, substantially reduces the mutation rates in MMR-defective mouse and human cells and conclude that high spontaneous mutation rates in MMR-defective cells are largely due to incorporation of oxidized dNTPs into DNA. In particular, the mutation rates of G:C-to-T:A transversions are reduced more than 30-fold by the over-expression. 2-OH-dATP is in general a poor substrate for mammalian DNA Pols [24]. Thus, the results shown in Fig. 1 together with the report by Russo et al. suggest that Polη may be involved in misincorporation of 2-OH-dATP opposite template G during DNA replication, thereby inducing G:C-to-T:A transversions in the MMR-defective cells. The incorporated 2-OH-A in DNA opposite template G may be recognized and removed by MMR. In fact, Egashira et al. [47] report that the frequency of G:C-to-T:A transversions in the spleen of *Mth1*$^{-/-}$ *Msh2*$^{-/-}$ mice is increased more than 30-fold compared to *Mth1*$^{-/-}$ mice. Thus, Polη may contribute to the induction of G:C-to-T:A transversions via incorporation of 2-OH-dATP opposite template G in the mouse and human cells.

In plus 8-OH-dGTP condition, addition of the oxidized dGTP increased the frequency of A-to-C transversions 17-fold during DNA synthesis (Fig. 1, Supplement Table 2). It indicates that h Polη inserts 8-OH-dGTP opposite template A with high efficiency (Fig. 5B). This is consistent with the kinetic data that suggest that h Polη incorporates 8-OH-dGTP opposite template A with almost as the incorporation of dTTP [31]. However, in the MMR-deficient cells, only three-fold reduction in the frequency of A:T-to-C:G transversions is observed associated with the over-expression of hMTH1 [19]. The frequency of A:T-to-C:G transversions in the *Mth1*$^{-/-}$ *Msh2*$^{-/-}$ mice was also increased about three-fold as compared to *Mth1*$^{-/-}$ mice [47]. Thus, the activity of Polη incorporating 8-OH-dGTP opposite template A may be attenuated in the mouse cells. The incorporated 8-OH-dGMP opposite template A might be excised by proofreading activities of other Pols [48].

Besides base substitutions, single-base frameshifts and large deletions with the size more than 100 bps were induced in plus 8-OH-dGTP condition (Figs. 2 and 3). This is in contrast to the spectra of mutations induced by the incorporation of 8-OH-dGTP into DNA by other Pols such as exo$^-$ *E. coli* Pol I, T4 and *Thermus thermophilus* Pols where only base substitutions are observed [48,49]. In the MMR-defective cells, hMTH1 expression also dramatically reduces single-base and dozens-base deletions, which indicate such frameshifts would be caused by misincorporation of oxidized purine dNTPs into DNA [19]. However, the reduction in single-base deletions by hMTH1 expression is mainly in a run of G whereas the increase in single-base deletions was in non-run sequences in the present study. Hence the contribution of Polη to the induction of the single-base deletions in the MMR-defective cells seems limited. In addition, no large deletions are observed in the MMR-defective cells and in the spleen of *Mth1*$^{-/-}$ *Msh2*$^{-/-}$ mice [47]. Thus, at present, relevance of frameshifts and large deletions observed in this study remains to be elucidated.

How are the single-base frameshifts and large deletions induced by incorporation of 8-OH-dGTP into DNA? We envisage that preference of h Polη incorporating 8-OH-dGTP into DNA could, at least in part, account for the mechanisms by which single-base frameshifts and large deletions are induced. This speculation is based on the facts that pyrimidines, i.e., T and C, in the template DNA were more frequently deleted than purines in the single-base frameshifts and that G was disfavored at 5′-side of the deleted bases (Fig. 2C, Table 3). The

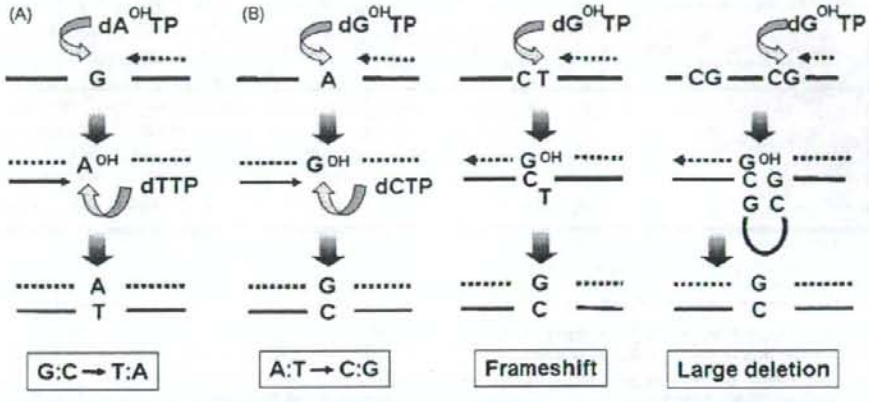

Fig. 5 – Proposed mechanisms by which various mutations are induced by incorporation of oxidized dNTPs into DNA by h Polη. (A) If 2-OH-dATP is incorporated opposite template G, and T is incorporated opposite 2-OH-A in the next round of DNA replication, G-to-T transversions will be induced (G:C → T:A). (B) If 8-OH-dGTP is incorporated opposite template A, and C is incorporated opposite 8-OH-G in the next round of DNA replication, A-to-C transversions will be induced (A:T → C:G). If 8-OH-dGTP is incorporated opposite template next C instead of correct T in 5′-GT-3′ sequences, one-bp deletion will be induced in the next round of DNA replication (frameshift). If h Polη stalls in GC-rich regions, i.e., nucleotides +165 to +169, and 8-OH-dGTP is incorporated opposite template C more than 100 bps downstream from the stalling site, large deletions will be induced in the next round of DNA replication (large deletion). Although this is not shown in the figure, if 8-OH-dGTP is incorporated opposite template C, and A is incorporated opposite 8-OH-G in the next round of DNA replication, C-to-A transversions will be induced (G:C → T:A).

hotspot of single-base frameshifts in plus 8-OH-dGTP condition is found in a sequence of 5′-CT-3′ where T was deleted eight times at nucleotide 137. Two moderate hotspots were also found in the sequence of 5′-CT-3′ where T was deleted four times at nucleotide 38 and three times at nucleotide 182. Thus, it seems that h Polη tends to incorporate 8-OH-dGTP opposite the adjacent C rather than T at the correct position, thereby inducing one-bp frameshifts (Fig. 5B). Since 5′-GX-3′ where X represents the deleted base was rare in the frameshifts, it probably disfavors incorporating 8-OH-dGTP opposite next G. This is basically consistent with the results of enzyme kinetics which indicate that h Polη poorly incorporates 8-OH-dGTP opposite template T and G [31]. The poor incorporation opposite template G might also contribute to the induction of large deletions because the regions where large deletions start and end, i.e., nucleotides −150 and −140 and nucleotides +165 to +169, respectively, are mostly GC-rich regions. We speculate that the h Polη may stall when it proceeds in the region nucleotides −150 and −140, which provides a chance to form secondary structures, i.e., more than 100 bps bulge in the template strand between the two regions. h Polη may skip over the bulge structures and restart DNA synthesis more than 100 bps downstream from the stalling site, thereby inducing deletions. The large active site of Polη that can accommodate bulky lesions might be the physical basis for the induction of frameshifts and large deletions associated with incorporation of 8-OH-dGTP into DNA [28].

Finally, we observed significant increases in MF compared to the control in the presence of low concentrations 8-OH-dGTP (Fig. 4, Supplement Table 3). The experiments were conducted because Tassotto and Mathews [50] failed to demonstrate the mutagenicity of 8-OH-dGTP at a concentration of 0.34 μM with HeLa cell extracts using the in vitro replication error detection system and raise the question of the role of 8-OH-dGTP in oxidative mutagenesis. Although we used purified Pol instead of cell extracts, which might contain less amounts of h Polη, the lowest concentration of 8-OH-dGTP where a significant increase in MF was observed was 0.2 μM, which was 1/1000 of that of the four normal dNTPs in the reaction mixture. To examine the significance of the increase in MFs at low concentrations of 8-OH-dGTP, we determined sequence changes of the mutants and calculated specific MFs of A-to-C transversions. However, the increases in specific MFs over the control level were not statistically significant. This may be due to the high background of mutations generated by Polη even without 8-OH-dGTP. Estimated concentration of normal dGTP in human cells is about 10 μM, and tumor cells have usually 5–10-fold higher concentrations of dGTP over normal cells [51]. Nonetheless, the results shown here are those obtained with in vitro experiments and thus additional work in vivo is required to estimate the role of Polη in induction of mutations at low concentrations of oxidized dNTPs.

In summary, we analyzed the mutations induced by incorporation of 2-OH-dATP and 8-OH-dGTP by h Polη using in vitro gap-filling assay. h Polη promotes G-to-T and A-to-C transversions in the presence of 2-OH-dATP and 8-OH-dGTP, respectively, and also promotes C-to-A transversions, one-base frameshifts and deletions with the size of more than 100 bps when 8-OH-dGTP was included in the reaction mixture. Since some of the mutations, e.g., G:C-to-T:A transversions, are observed in cells where oxidized dNTPs play important roles in mutagenesis [19,47], we suggest that h Polη may be

involved in a variety of mutations in human cells by efficient and erroneous incorporation of oxidized dNTPs into DNA. It is reported, however, that extracts of XP-V cells deficient in h Polη exhibit similar capacity to induce mutations with 8-OH-dGTP and 2-OH-dATP in an in vitro DNA replication system to those of HeLa cells [52]. Other Pols also have a potential to induce A-to-C transversions by incorporation of 8-OH-dGTP into DNA in vitro [48]. Thus, further work is needed to examine the cellular roles of h Polη to induce oxidative mutations by incorporation of oxidized dNTPs into DNA in human cells.

Acknowledgements

We thank Dr. Thomas A. Kunkel, NIEHS, USA, for providing bacteriophage and E. coli. This work is supported by grants-in-aid for scientific research from the Ministry of Education, Culture, Sports, Science and Technology, Japan (MEXT), the Ministry of Health, Labour and Welfare, Japan (MHLW) and the Japan Health Science Foundation (JHSF). This work was also supported by grants-in-aid for international collaborative research (SH34407) from JHSF, cancer research from MHLW and nuclear research from MEXT, based on the screening and counseling by the Atomic Energy Commission.

Appendix A. Supplementary data

Supplementary data associated with this article can be found, in the online version, at doi:10.1016/j.dnarep.2007.12.005.

REFERENCES

[1] S. Bjelland, E. Seeberg, Mutagenicity, toxicity and repair of DNA base damage induced by oxidation, Mutat. Res. 531 (2003) 37–80.
[2] H. Kamiya, Mutagenic potentials of damaged nucleic acids produced by reactive oxygen/nitrogen species: approaches using synthetic oligonucleotides and nucleotides: survey and summary, Nucleic Acids Res. 31 (2003) 517–531.
[3] B.N. Ames, Dietary carcinogens and anticarcinogens. Oxygen radicals and degenerative diseases, Science 221 (1983) 1256–1264.
[4] A.L. Jackson, L.A. Loeb, The contribution of endogenous sources of DNA damage to the multiple mutations in cancer, Mutat. Res. 477 (2001) 7–21.
[5] M. Sekiguchi, T. Tsuzuki, Oxidative nucleotide damage: consequences and prevention, Oncogene 21 (2002) 8895–8904.
[6] M.L. Michaels, J.H. Miller, The GO system protects organisms from the mutagenic effect of the spontaneous lesion 8-hydroxyguanine (7,8-dihydro-8-oxoguanine), J. Bacteriol. 174 (1992) 6321–6325.
[7] Y. Nakabeppu, K. Sakumi, K. Sakamoto, D. Tsuchimoto, T. Tsuzuki, Y. Nakatsu, Mutagenesis and carcinogenesis caused by the oxidation of nucleic acids, Biol. Chem. 387 (2006) 373–379.
[8] H. Maki, M. Sekiguchi, MutT protein specifically hydrolyses a potent mutagenic substrate for DNA synthesis, Nature 355 (1992) 273–275.
[9] C. Yanofsky, E.C. Cox, V. Horn, The unusual mutagenic specificity of an E. Coli mutator gene, Proc. Natl. Acad. Sci. U. S. A 55 (1966) 274–281.
[10] H. Kasai, Chemistry-based studies on oxidative DNA damage: formation, repair, and mutagenesis, Free Radic. Biol. Med. 33 (2002) 450–456.
[11] A. Sakai, M. Nakanishi, K. Yoshiyama, H. Maki, Impact of reactive oxygen species on spontaneous mutagenesis in *Escherichia coli*, Genes Cells 11 (2006) 767–778.
[12] M. Inoue, H. Kamiya, K. Fujikawa, Y. Ootsuyama, N. Murata-Kamiya, T. Osaki, K. Yasumoto, H. Kasai, Induction of chromosomal gene mutations in *Escherichia coli* by direct incorporation of oxidatively damaged nucleotides. New evaluation method for mutagenesis by damaged DNA precursors in vivo, J. Biol. Chem. 273 (1998) 11069–11074.
[13] H. Kamiya, H. Kasai, 2-Hydroxy-dATP is incorporated opposite G by *Escherichia coli* DNA polymerase III resulting in high mutagenicity, Nucleic Acids Res. 28 (2000) 1640–1646.
[14] H. Kamiya, E. Iida, N. Murata-Kamiya, Y. Yamamoto, T. Miki, H. Harashima, Suppression of spontaneous and hydrogen peroxide-induced mutations by a MutT-type nucleotide pool sanitization enzyme, the *Escherichia coli* Orf135 protein, Genes Cells 8 (2003) 941–950.
[15] H. Kamiya, N. Murata-Kamiya, E. Iida, H. Harashima, Hydrolysis of oxidized nucleotides by the *Escherichia coli* Orf135 protein, Biochem. Biophys. Res. Commun. 288 (2001) 499–502.
[16] T. Tsuzuki, A. Egashira, H. Igarashi, T. Iwakuma, Y. Nakatsuru, Y. Tominaga, H. Kawate, K. Nakao, K. Nakamura, F. Ide, S. Kura, Y. Nakabeppu, M. Katsuki, T. Ishikawa, M. Sekiguchi, Spontaneous tumorigenesis in mice defective in the MTH1 gene encoding 8-oxo-dGTPase, Proc. Natl. Acad. Sci. U. S. A 98 (2001) 11456–11461.
[17] K. Fujikawa, H. Kamiya, H. Yakushiji, Y. Fujii, Y. Nakabeppu, H. Kasai, The oxidized forms of dATP are substrates for the human MutT homologue, the hMTH1 protein, J. Biol. Chem. 274 (1999) 18201–18205.
[18] C. Colussi, E. Parlanti, P. Degan, G. Aquilina, D. Barnes, P. Macpherson, P. Karran, M. Crescenzi, E. Dogliotti, M. Bignami, The mammalian mismatch repair pathway removes DNA 8-oxodGMP incorporated from the oxidized dNTP pool, Curr. Biol. 12 (2002) 912–918.
[19] M.T. Russo, M.F. Blasi, F. Chiera, P. Fortini, P. Degan, P. Macpherson, M. Furuichi, Y. Nakabeppu, P. Karran, G. Aquilina, M. Bignami, The oxidized deoxynucleoside triphosphate pool is a significant contributor to genetic instability in mismatch repair-deficient cells, Mol. Cell Biol. 24 (2004) 465–474.
[20] T. Nohmi, S.R. Kim, M. Yamada, Modulation of oxidative mutagenesis and carcinogenesis by polymorphic forms of human DNA repair enzymes, Mutat. Res. 591 (2005) 60–73.
[21] H.J. Einolf, F.P. Guengerich, Fidelity of nucleotide insertion at 8-oxo-7,8-dihydroguanine by mammalian DNA polymerase delta. Steady-state and pre-steady-state kinetic analysis, J. Biol. Chem. 276 (2001) 3764–3771.
[22] H.J. Einolf, N. Schnetz-Boutaud, F.P. Guengerich, Steady-state and pre-steady-state kinetic analysis of 8-oxo-7,8-dihydroguanosine triphosphate incorporation and extension by replicative and repair DNA polymerases, Biochemistry 37 (1998) 13300–13312.
[23] H. Miller, R. Prasad, S.H. Wilson, F. Johnson, A.P. Grollman, 8-oxodGTP incorporation by DNA polymerase beta is modified by active-site residue Asn279, Biochemistry 39 (2000) 1029–1033.
[24] H. Kamiya, H. Kasai, Formation of 2-hydroxydeoxyadenosine triphosphate, an oxidatively damaged nucleotide, and its incorporation by DNA polymerases. Steady-state kinetics of the incorporation, J. Biol. Chem. 270 (1995) 19446–19450.
[25] H. Ohmori, E.C. Friedberg, R.P. Fuchs, M.F. Goodman, F. Hanaoka, D. Hinkle, T.A. Kunkel, C.W. Lawrence, Z. Livneh, T. Nohmi, L. Prakash, S. Prakash, T. Todo, G.C. Walker, Z. Wang,

R. Woodgate, The Y-family of DNA polymerases, Mol. Cell 8 (2001) 7–8.
[26] C. Masutani, R. Kusumoto, A. Yamada, N. Dohmae, M. Yokoi, M. Yuasa, M. Araki, S. Iwai, K. Takio, F. Hanaoka, The XPV (xeroderma pigmentosum variant) gene encodes human DNA polymerase η, Nature 399 (1999) 700–704.
[27] R.E. Johnson, S. Prakash, L. Prakash, Efficient bypass of a thymine–thymine dimer by yeast DNA polymerase, Polη, Science 283 (1999) 1001–1004.
[28] S. Prakash, R.E. Johnson, L. Prakash, Eukaryotic translesion synthesis DNA polymerases: specificity of structure and function, Ann. Rev. Biochem. 74 (2005) 317–353.
[29] E.C. Friedberg, Suffering in silence: the tolerance of DNA damage, Nat. Rev. Mol. Cell Biol. 6 (2005) 943–953.
[30] T. Nohmi, Environmental stress and lesion-bypass DNA polymerases, Ann. Rev. Microbiol. 60 (2006) 231–253.
[31] M. Shimizu, P. Gruz, H. Kamiya, C. Masutani, Y. Xu, Y. Usui, H. Sugiyama, H. Harashima, F. Hanaoka, T. Nohmi, Efficient and erroneous incorporation of oxidized DNA precursors by human DNA polymerase eta, Biochemistry 46 (2007) 5515–5522.
[32] M. Shimizu, P. Gruz, H. Kamiya, S.R. Kim, F.M. Pisani, C. Masutani, Y. Kanke, H. Harashima, F. Hanaoka, T. Nohmi, Erroneous incorporation of oxidized DNA precursors by Y-family DNA polymerases, EMBO Rep. 4 (2003) 269–273.
[33] M. Yamada, T. Nunoshiba, M. Shimizu, P. Gruz, H. Kamiya, H. Harashima, T. Nohmi, Involvement of Y-family DNA polymerases in mutagenesis caused by oxidized nucleotides in Escherichia coli, J. Bacteriol. 188 (2006) 4992–4995.
[34] K. Bebenek, T.A. Kunkel, Analyzing fidelity of DNA polymerases, Methods Enzymol. 262 (1995) 217–232.
[35] P. Kannouche, B.C. Broughton, M. Volker, F. Hanaoka, L.H. Mullenders, A.R. Lehmann, Domain structure, localization, and function of DNA polymerase η, defective in xeroderma pigmentosum variant cells, Genes Dev. 15 (2001) 158–172.
[36] A. Tissier, P. Kannouche, M.P. Reck, A.R. Lehmann, R.P. Fuchs, A. Cordonnier, Co-localization in replication foci and interaction of human Y-family members, DNA polymerase polη and REV1 protein, DNA Repair (Amst.) 3 (2004) 1503–1514.
[37] C. Masutani, R. Kusumoto, S. Iwai, F. Hanaoka, Mechanisms of accurate translesion synthesis by human DNA polymerase eta, EMBO J. 19 (2000) 3100–3109.
[38] T. Matsuda, K. Bebenek, C. Masutani, F. Hanaoka, T.A. Kunkel, Low fidelity DNA synthesis by human DNA polymerase-eta, Nature 404 (2000) 1011–1013.
[39] T. Matsuda, K. Bebenek, C. Masutani, I.B. Rogozin, F. Hanaoka, T.A. Kunkel, Error rate and specificity of human and murine DNA polymerase eta, J. Mol. Biol. 312 (2001) 335–346.
[40] A.R. Lehmann, New functions for Y family polymerases, Mol. Cell 24 (2006) 493–495.
[41] M.J. McIlwraith, A. Vaisman, Y. Liu, E. Fanning, R. Woodgate, S.C. West, Human DNA polymerase eta promotes DNA synthesis from strand invasion intermediates of homologous recombination, Mol. Cell 20 (2005) 783–792.
[42] T. Kawamoto, K. Araki, E. Sonoda, Y.M. Yamashita, K. Harada, K. Kikuchi, C. Masutani, F. Hanaoka, K. Nozaki, N. Hashimoto, S. Takeda, Dual roles for DNA polymerase eta in homologous DNA recombination and translesion DNA synthesis, Mol. Cell 20 (2005) 793–799.
[43] V.I. Mayorov, I.B. Rogozin, L.R. Adkison, P.J. Gearhart, DNA polymerase eta contributes to strand bias of mutations of A versus T in immunoglobulin genes, J. Immunol. 174 (2005) 7781–7786.
[44] V.G. Godoy, D.F. Jarosz, F.L. Walker, L.A. Simmons, G.C. Walker, Y-family DNA polymerases respond to DNA damage-independent inhibition of replication fork progression, EMBO J. 25 (2006) 868–879.
[45] S. de Feraudy, C.L. Limoli, E. Giedzinski, D. Karentz, T.M. Marti, L. Feeney, J.E. Cleaver, Pol eta is required for DNA replication during nucleotide deprivation by hydroxyurea, Oncogene 26 (2007) 5713–5721.
[46] K. Bebenek, T. Matsuda, C. Masutani, F. Hanaoka, T.A. Kunkel, Proofreading of DNA polymerase eta-dependent replication errors, J. Biol. Chem. 276 (2001) 2317–2320.
[47] A. Egashira, K. Yamauchi, K. Yoshiyama, H. Kawate, M. Katsuki, M. Sekiguchi, K. Sugimachi, H. Maki, T. Tsuzuki, Mutational specificity of mice defective in the MTH1 and/or the MSH2 genes, DNA Repair (Amst.) 1 (2002) 881–893.
[48] Y.I. Pavlov, D.T. Minnick, S. Izuta, T.A. Kunkel, DNA replication fidelity with 8-oxodeoxyguanosine triphosphate, Biochemistry 33 (1994) 4695–4701.
[49] K.C. Cheng, D.S. Cahill, H. Kasai, S. Nishimura, L.A. Loeb, 8-Hydroxyguanine, an abundant form of oxidative DNA damage, causes G to T and A to C substitutions, J. Biol. Chem. 267 (1992) 166–172.
[50] M.L. Tassotto, C.K. Mathews, Assessing the metabolic function of the MutT 8-oxodeoxyguanosine triphosphatase in Escherichia coli by nucleotide pool analysis, J. Biol. Chem. 277 (2002) 15807–15812.
[51] T.W. Traut, Physiological concentrations of purines and pyrimidines, Mol. Cell Biochem. 140 (1994) 1–22.
[52] K. Satou, H. Kasai, C. Masutani, F. Hanaoka, H. Harashima, H. Kamiya, 2-Hydroxy-2′-deoxyadenosine 5′-triphosphate enhances A·T->C·G mutations caused by 8-hydroxy-2′-deoxyguanosine 5′-triphosphate by suppressing its degradation upon replication in a HeLa extract, Biochemistry 46 (2007) 6639–6646.

DNA Repair and DNA Damage Tolerance in Archaeal Bacteria: Extreme Environments and Genome Integrity

7

Takehiko Nohmi, Masami Yamada and Petr Gruz

Abstract

Maintenance of genome integrity is a mechanism central to cellular life. Many Archaeal species live in harsh habitats that are extreme challenges to genome stability. In the habitat at high ambient temperatures, deamination, oxidation and depurination are greatly accelerated and various lesions are supposed to accumulate in the genomic DNA. Thus, the organisms living in such extreme conditions seem to evolve novel strategies for repairing DNA damage and avoiding mutations caused by the lesions. In this chapter, we review mechanisms of DNA repair in archaeal Bacteria and unique properties of archaeal DNA polymerases (Pols) to tolerate DNA damage. In general, archaeal DNA repair proteins are eukaryote-like although many counterparts are missing in the genome sequences. Archaeal B-family DNA Pols, such as *Sso* DNA Pol B1 or *Pfu*, halt DNA replication several basepairs before template uracil or hypoxanthine, deamination products of cytosine or adenine in template DNA, respectively, thereby apparently avoiding mutations (read-ahead mechanism). Fifteen out of 38 archaeal species whose genome sequences have been completely determined seem to possess Y-family DNA Pols, which are specialized to bypass lesions in DNA. Collectively, these molecular features warrant the future investigation on how Archaea accommodate DNA damage inevitably occurring in the extreme harsh environments.

Introduction

Archaea, the third domain of life, is thought to possess pathways involved in DNA replication, repair, recombination and transcription, similar to those of Eukarya, although its morphology is more prokaryotic-like (Olsen and Woese, 1996). Many eukaryotic repair proteins have close homologues in Archaea and thus archaeal proteins have been utilized as structural and biochemical models to reveal the mechanisms of action of the eukaryotic counterparts because of their structural stability and ease of purification. However, DNA-repair pathways in Archaea themselves are not yet well characterized, and several important counterparts are apparently missing in the Archaeal genome, suggesting that Archaea may possess unique mechanisms to protect the genome. This may not be surprising given the environmental challenges faced by hyperthermophilic Archaea living in habitats at extremely high temperatures. Chemical reactions such as hydrolytic deamination are greatly accelerated at high temperatures so that the hyperthermophilic organisms are supposed to be exposed to massive DNA damages. In addition, most of proteins and nucleic acids are denatured at high temperatures. Nevertheless, the mutation frequencies in hyperthermophilic Archaea, i.e. *Sulfolobus acidocaldarius*, are comparable with or lower than those of other microorganisms such as *Escherichia coli* (Grogan *et al.*, 2001). Thus, Archaea seem to have evolved unique and efficient mechanisms to protect their genome from harsh environmental conditions.

In addition to DNA repair, B-family DNA polymerases (DNA Pols) in the hyperthermophic Archaea have a unique property that they halt replication once they encounter uracil (U) or hypoxanthine (HX), which are

deamination products of cytosine and adenine, respectively, in the template genome (Fogg *et al.*, 2002; Gruz *et al.*, 2003). Because they stall several basepairs before the lesions, it is called 'read-ahead mechanism' (Greagg *et al.*, 1999). This is regarded as an error avoidance mechanism in hyperthermophilic Archaea because the stalling of DNA replication provides a chance to remove the deaminated bases from the template DNA strands. The molecular feature is unique in hyperthermophic Archaea since DNA Pols from thermophilic eubacteria such as *Taq* DNA Pol do not share similar properties. Besides B-family DNA Pols, which are responsible for chromosome replication, 15 out of 38 archaeal species whose genome sequences have been completed seem to possess Y-family DNA Pols (Ohmori *et al.*, 2001). The Y-family represents a novel family of DNA Pols found in Archaea, Bacteria and Eukarya, and the most remarkable feature is that they can bypass a variety of DNA lesions efficiently (Prakash *et al.*, 2005; Nohmi, 2006). Thus, they are involved in tolerance to DNA damage induced by exogenous and endogenous genotoxic agents. In this chapter, we review unique mechanisms of DNA repair and damage tolerance in Archaea and discuss the future directions.

DNA repair

DNA repair is the molecular mechanism that removes various damages in DNA, thereby ensuring the genome integrity. In fact, all organisms from virus to humans including Archaea are equipped with multiple DNA repair machineries to counteract the genotoxic damage. DNA lesions are induced by exposure to hazardous environmental factors, e.g. sunlight, and endogenous mutagens produced during oxygen consumption and nutritional metabolism, e.g. reactive oxygen species and alkylating agents. Deficit of DNA repair leads to hypersensitivity to toxic and mutagenic effects of genotoxic hazards as has been exemplified by the presence of human genetic diseases such as xeroderma pigmentosum (XP) (Tanaka *et al.*, 1990). The XP patients are sensitive to sun light-induced skin cancer because of the deficit of the ability to remove cyclobutane pyrimidine dimers (CPD) from DNA. In the following section, we view six most important pathways of DNA repair: alkylation repair; photorepair; nucleotide excision repair (NER); base excision repair (BER); mismatch repair (MMR) and homologous recombination (HR) in Archaea (Fig. 7.1, Table 7.1). Of these, alkylation repair and photorepair directly reverse the damages while NER, BER and MMR require multiple steps to remove the damaged or mismatched bases, followed by resynthesis of DNA to fill in the gaps. HR as well as translesion DNA synthesis (TLS), which will be described in detail below, does not remove DNA damage but rescues the stalled DNA replication to complete the duplication of chromosome DNA (damage avoidance). Most Archaea as well as Bacteria and Eukarya have multiple, functionally redundant pathways to combat a variety of damages in DNA induced by environmental stress.

Repair of alkylation damage

DNA repair protein O^6-alkylguanine-DNA alkyltransferase (AGT) is considered to play central roles in the mechanism of cellular resistance to the toxic and mutagenic effects of DNA damage induced by monofunctional alkylating agents (Sedgwick, 2004; Lindahl *et al.*, 1988). AGT operates by the transfer of the offending alkyl groups from the O^6 position of guanine and the O^4 position of thymine in DNA to a cysteine residue at the active site of the protein. This is an irreversible process that results in the stoichiometric inactivation of the protein, the repair of other lesions requiring additional active molecules. The alkylation damage to DNA occurs under a variety of living conditions because alkylating agents including *N*-nitroso compounds are present in the environment and can be generated even endogenously (Taverna and Sedgwick, 1996). The AGT proteins share a highly conserved -PCHRV- amino acid sequence in their active site (Margison *et al.*, 2003). The presence of an AGT gene product or a putative gene has been reported so far in c.a. 100 different species from the three domains of life.

It is shown that extracts of two Crenarchaeota, i.e. *Sulfolobus acidocaldarius* and *Pyrobaculum islandicum*, and two Euryarchaota, i.e. *Pyrococcus furiosus* and *Thermococcus litoralis*, contain the AGT activities (Skorvaga *et al.*,